The European Zoological Journal

ISSN: (Print) (Online) Journal homepage: https://www.tandfonline.com/loi/tizo21

Morphology and taxonomy of the genus *Ramazzottius* (Eutardigrada; Ramazzottiidae) with the integrative description of *Ramazzottius kretschmanni* sp. nov

R. Guidetti, M. Cesari, I. Giovannini, C. Ebel, M. I. Förschler, L. Rebecchi & R. O. Schill

To cite this article: R. Guidetti, M. Cesari, I. Giovannini, C. Ebel, M. I. Förschler, L. Rebecchi & R. O. Schill (2022) Morphology and taxonomy of the genus *Ramazzottius* (Eutardigrada; Ramazzottiidae) with the integrative description of *Ramazzottius kretschmanni* sp. nov, The European Zoological Journal, 89:1, 339-363, DOI: 10.1080/24750263.2022.2043468

To link to this article: https://doi.org/10.1080/24750263.2022.2043468

The European Zoological Journal, 2022, 339–363
Vol. 89, No. 1, https://doi.org/10.1080/24750263.2022.2043468

Morphology and taxonomy of the genus *Ramazzottius* (Eutardigrada; Ramazzottiidae) with the integrative description of *Ramazzottius kretschmanni* sp. nov.

R. GUIDETTI [1], M. CESARI [1], I. GIOVANNINI[1], C. EBEL[2], M. I. FÖRSCHLER[3], L. REBECCHI [1], & R. O. SCHILL[4]

[1]*Department of Life Sciences, University of Modena and Reggio Emilia, Modena, Italy,* [2]*Department Visitor Information, Black Forest National Park, Seebach, Germany,* [3]*Department of Ecosystem Monitoring, Research and Conservation. Black Forest National Park, Freudenstadt, Germany, and* [4]*Institute of Biomaterials and Biomolecular Systems, University of Stuttgart, Stuttgart, Germany*

(Received 20 October 2021; accepted 11 February 2022)

Abstract
The species of the genus *Ramazzottius* (Ramazzottiidae, Eutardigrada) are among the most common and widespread tardigrade species in the world. Most of the 28 *Ramazzottius* species have been described only with morphological characters which were most of the time represented only with drawings. The discovery of a new species of this genus in the Black Forest (Germany) provided the opportunity to compare this species with the type specimens of ten *Ramazzottius* species, to propose the status of *species dubia* for *Ramazzottius edmondabouti*, and through new photographs to elucidate the anatomy of animals and eggs (in particular of the head sensory regions, eye spots, buccal tube, ornamentations of the dorsal posterior cuticle, and morphology of egg processes). These thorough observations led to a better understanding of the diversity and evolution, not only of this cosmopolitan genus, but also of other eutardigrade genera. The new species *Ramazzottius kretschmanni* is described with an integrative approach integrating morphological (light and electron microscopy observations and morphometric data) and molecular (*cox1* and ITS2 genes) data. The PTP and ASAP analyses confirmed the validity of the new species from a molecular point of view. The new species is morphologically similar to *Ramazzottius oberhaeuseri*, but is distinguishable by the smooth cuticle, the presence of a "cheek-like" area on the head, and the size of egg processes as well as different sequences of the molecular markers.

Keywords: Ramazzottius kretschmanni *sp. nov.*, *sensory regions, black forest, cuticle ornamentations, eye spots*

Introduction

With the introduction of molecular characterization of tardigrade species (Schill & Steinbrück 2007; Cesari et al. 2009; Schill et al. 2010; Wełnicz et al. 2011), the integrative description of taxa has become quite common in Tardigrada in recent years (e.g. Kaczmarek et al. 2020; Kihm et al. 2020; Morek et al. 2020a; Nelson et al. 2020; Stec et al. 2020a, 2020b; Tumanov 2020; Guidetti et al. 2021; Massa et al. 2021). The integration of data from different sources (e.g. morphological and morphometric traits, nucleotide sequences, reproductive modes, karyotype) led to a more accurate definition of tardigrade species, also with the identification of pseudocryptic or cryptic species (e.g. Faurby et al. 2008; Guil & Giribet 2009; Gąsiorek et al. 2019; Santos et al. 2019; Guidetti et al. 2019a; Stec et al. 2021). One of the tardigrade genera in which cryptic/pseudocryptic species were found is *Ramazzottius* Binda & Pilato, 1986 (Faurby et al. 2008; Pilato et al. 2013; Stec et al. 2018). The species of this genus are among the most common and widespread tardigrades in the world and are found mainly in xeric mosses and lichens (McInnes 1994; Kaczmarek et al. 2014, 2015, 2016; McInnes et al.

Correspondence: M. Cesari, Department of Life Sciences, University of Modena and Reggio Emilia, Via G. Campi 213/D, 41125 Modena, Italy. Email: michele.cesari@unimore.it

2017). Erected by Binda and Pilato (1986), *Ramazzottius* contains 28 species (Degma et al. 2021), including the type species *Ramazzottius oberhaeuseri* (Doyère, 1840), one of the first tardigrade species ever described, and previously considered cosmopolitan until its redescription (Stec et al. 2018).

Within this genus, only two species have been described with an integrative approach: *R. oberhaeuseri* (the neotype population; Stec et al. 2018) and *Ramazzottius sabatiniae* Guidetti, Massa, Bertolani, Rebecchi & Cesari, 2019b. All the other species were described only by morphological and morphometric characters using Light Microscopy [LM], plus Scanning Electron Microscopy [SEM] for only five of them (Kaczmarek et al. 2006; Dastych 2011; Stec et al. 2017, 2018; Guidetti et al. 2019b). In the papers in which *Ramazzottius* species are described, the morphological characters are illustrated with photos (not always of good quality) in only half of them, and for 13 species, animals and eggs morphologies are represented only by drawings. The drawings can be useful because they can reproduce multifocal images of a structure/character and can emphasize the details useful for taxonomic identification. On the other hand, drawings are not objective representations, as they are subjected to the interpretation of authors, who may neglect details that could be useful for species comparisons.

The discovery of a new *Ramazzottius* species from the Black Forest in Germany provided the opportunity to compare this species with the type specimens of several *Ramazzottius* species, to take new photographs of these specimens elucidating the anatomy of animals and eggs, and to develop a better understanding of the diversity and evolution not only of this cosmopolitan genus but also of other eutardigrade genera.

Material and methods

Tardigrade sampling and morphological analyses

Tardigrades were extracted from a moss growing on tree bark (C4322-Probe103) collected in October 2016 by Ralph O. Schill in the Black Forest (Schwarzwald, Germany). These specimens were morphologically analyzed with LM, and those belonging to a new species were also analysed with SEM or characterized with a molecular approach.

To extract tardigrades, fragments of the moss sample were placed in distilled water for about half an hour. After soaking, the sample was sieved (sieve meshes: 500 μm and 38 μm) to separate tardigrades and eggs from the substrate. Animals and eggs were then isolated using a needle, removed with a glass pipette under a stereomicroscope, and mounted on slides in Hoyer's medium. Specimens for SEM observations were fixed in boiling absolute ethanol for few minutes, then were rinsed three times in absolute ethanol, desiccated by evaporation, mounted on stubs, and sputter coated with gold. Observations with SEM were carried out with EVO-LS 10 (Carl Zeiss company), available at the Institute of Evolution and Ecology at the University of Tübingen (Germany).

Observations with LM and measurements were carried out under both phase contrast [PhC] and differential interference contrast [DIC] up to the maximum magnification (100× oil objective) with a Leica DM RB microscope equipped with a Nikon DS-Fi 1 or an AmScope MU1803 digital cameras, at the Department of Life Sciences, University of Modena and Reggio Emilia (UNIMORE), Italy. Measurements of the lengths of the animals and their cuticular structures (*i.e.* claws, structures of feeding apparatus) were made according to Kaczmarek and Michalczyk (2017) and Stec et al. (2018); structures were measured only if they were in proper position. Morphometric data were handled using the "Parachela" ver. 1.6 template available from the Tardigrada Register (Michalczyk & Kaczmarek 2013), updated with the Thorpe's normalization of the data (as in Massa et al. 2021) according to Bartels et al. (2011a).

As comparative material the following type specimens were observed with LM: *Ramazzottius affinis* Bertolani, Guidetti & Rebecchi, 1994 (holotype, slide 1546s7; egg, 1527s27), *Ramazzottius andreevi* Biserov, 1997/98 (paratype+egg, slide 1964–9), *Ramazzottius sabatiniae* (holotype, slide C4203s7), *Ramazzottius semisculptus* Pilato & Rebecchi, 1992 (paratypes, slide 47s14), *Ramazzottius tribulosus* Bertolani & Rebecchi, 1988 (holotype, slide 901s32; egg, 793s23), *Ramazzottius valaamis* Biserov & Tumanov, 1993 (paratype+egg, slide 1518–5), *Ramazzottius varieornatus* Bertolani & Kinchin, 1993 (holotype, slide 1370s48), all from the Bertolani Collection (Department of Life Sciences, UNIMORE); *Ramazzottius anomalus* (Ramazzotti, 1962a) (sintype+egg, slide 5951), *Ramazzottius subanomalus* (Biserov, 1985) (paratype+egg, slide 12,890), all from the Maucci Collection (Natural History Museum of Verona, Italy); *R. andreevi* (holotype, slide 1964(2); paratype 1964), *Ramazzottius caucasicus* Biserov, 1997/98 (holotype, slide 218(14); paratypes+egg, slide 218–15), *Ramazzottius rupeus* Biserov, 1999 (holotype, slide 2236(6); paratypes+egg, slide 2236(2), *R. subanomalus* (holotype+egg, slide 200(15)), *R. valaamis* (holotype, slide 1518–1; paratype egg,

slide 1518), all from the Biserov Collection (Natural History Museum of Verona, Italy); *R. semisculptus* (holotype, slide 4192), *Ramazzottius thulini* (Pilato, 1970) (holotype, slide 917), both from the Binda & Pilato Collection (Department of Biological, Geological, and Environmental Sciences, University of Catania, Italy).

Molecular characterization

Prior to the molecular analysis, individuals were observed and identified with LM using the method described in Cesari et al. (2011) to obtain photo voucher specimens. Genomic DNA was extracted from four separate animals. The extractions were performed with QuickExtract™ DNA Extraction Solution (Lucigen), following the manufacturer's protocol. Investigations of molecular genetic markers were carried out using fragments of mitochondrial (cytochrome c oxidase subunit 1: *cox1*) and nuclear (internal transcribed spacer 2: ITS2) genes. The *cox1* gene was amplified using primers and PCR protocols described in Cesari et al. (2009) (*cox1*, Forward: LCO 5'-GGT CAA CAA ATC ATA AAG ATA TTG G-3', Reverse: HCOoutout 5'-CCT GGT AAA ATR AGA ATA TAR-3'; amplicon length: 549). The ITS2 was amplified utilizing primers and PCR protocols described in Wełnicz et al. (2011) (ITS2, Forward: ITS3 5'-GCA TCG ATG AAG AAC GCA G-3', Reverse: ITS4 5'-AGT TTY TTT TCC TCC GCT TA-3'; amplicon length; 501). The amplified products were gel purified using the Wizard Gel and PCR cleaning (Promega, Madison, WI, USA) kit. Sequencing reactions were performed using the ABI Prism Big Dye Terminator v. 1.1 Sequencing Kit (Applied Biosystems™) on purified amplicons. Each sequencing reaction contained 0.2 μM of a single PCR primer to initiate the sequencing reaction, 2 μL of BigDye, 70 ng of purified products, 4 μL of 5x BigDye Terminator v.1.1 Sequencing Buffer and H_2O for a final volume of 20 μL. Cycling conditions for sequencing reactions consisted of 25 cycles of 96°C for 10s, 50°C for 5s and 60°C for 4 min. Both strands were sequenced with ABI Prism 3100 (Applied Biosystems™). Nucleotide sequences of the newly analyzed specimens were submitted to GenBank, the accession numbers for *cox1* of the four sequenced specimens (C4322 T1-T4) are OM370801-04, for ITS2 are OM402517-20.

The *cox1* and ITS2 nucleotide sequences were aligned with the MAFFT algorithm (Katoh et al. 2002) as implemented in the MAFFT online service (Katoh et al. 2017) and checked by visual inspection. For *cox1* sequences, chromatograms were checked for presence of ambiguous bases, as sequences were translated to amino acids by using the invertebrate mitochondrial code implemented in MEGA X (Kumar et al. 2018) to check for the presence of stop codons and therefore of pseudogenes. Sequences of other tardigrade sequences from GenBank belonging to *Ramazzottius* species were also included in the analysis for comparisons (Tab. S1 Supporting information). Pairwise nucleotide sequence divergences between sequences were calculated using p-distance with MEGA X for each gene.

Furthermore, relationships between *cox1* and ITS2 were estimated using a parsimony network, by applying the method described in Templeton et al. (1992), as implemented in TCS ver. 1.21 (Clement et al. 2000) and visualized using tcsBU (Múrias Dos Santos et al. 2016). A 95% connection limit was employed, as it has been suggested as a useful general tool in species assignments and discovery (Hart & Sunday 2007). Putative species were also inferred by using the Poisson Tree Process (PTP; Zhang et al. 2013) and the Assemble Species by Automatic Partitioning method (ASAP; Puillandre et al. 2021). The PTP method produces robust species diversity estimates, and the starting gene trees were maximum likelihood (ML) trees computed using RAxML ver. 7.2.4 (Stamatakis 2006), as implemented in CIPRES (Miller et al. 2010), under the GTR+G model, as inferred by using the Akaike Information Criterion on jModelTest2 (Guindon & Gascuel 2003; Darriba et al. 2012) for both genes. Sequences of *Hypsibius convergens* (Urbanowicz, 1925) (GenBank accession number: FJ435798) and *Hypsibius exemplaris* Gąsiorek, Stec, Morek & Michalczyk, 2018 (GenBank accession number: MG800336) were used as outgroups for the genes *cox1* and ITS2, respectively. Bootstrap resampling with 1000 replicates was undertaken via the rapid bootstrap procedure of Stamatakis et al. (2008) to assign support to branches in the ML tree. Bayesian trees were also computed using different models as inferred by MrModeltest ver. 2 (Nylander 2004). For the *cox1* gene, the following models were utilized to consider the different evolutionary models for the three codons: SYM+I+G for the first position of the codon, GTR for the second position of the codon and GTR+G for the third position of the codon; while for the ITS2 gene the model HKY+G was utilized. The Bayesian dendrograms was computed with the program MrBayes ver. 3.2.7a (Huelsenbeck & Ronquist 2001; Ronquist & Huelsenbeck 2003), as implemented in CIPRES. Two independent runs, each of four Metropolis

coupled Markov chains Monte Carlo method, were launched for 3×10^7 generations, and trees were sampled every 1000 generations. Convergence of runs was assessed by tracking average standard deviation of split frequencies between runs and by plotting the log likelihood of sampled trees in TRACER ver. 1.7 (Rambaut et al. 2018) and the first 3×10^6 sampled generations were discarded as burn-in. In the distance-based ASAP method, the sequences are sorted into hypothetical species based on the barcode gap (i.e. whenever the divergence among organisms belonging to the same species is smaller than divergence among organisms from different species). The method first detects the barcode gap as the first significant gap beyond a model-based one-sided confidence limit for intraspecific divergence, and then uses it to produce several partitions of the data. The ASAP then computes an *ad hoc* ASAP-score for each defining partition, with the lower score indicating the better partition. The analysis was performed on the ASAP website (https://bioinfo.mnhn.fr/abi/public/asap/).

Results

Comparisons of the new species with type specimens of several *Ramazzottius* species provided the opportunity to describe characteristics not reported in the original descriptions of those species and to obtain new photographs of several characters, not always present in the original papers. The new species description and the comparisons are provided below.

Ramazzottius kretschmanni sp. nov. **(Figures 1–4; Tables I, *S2)***

ZOOBANK: urn: lsid:zoobank.org:pub: 2F52B05A-7353-49B9-A6B6-0B8F818FD9C2

Holotype. slide C4322s6-Probe103.

Paratypes. 45 animals and 21 eggs mounted on slides, 10 animals and 3 eggs mounted on stubs for SEM observations.

Type repositories. the holotype (C4322s6-Probe103) and 20 paratypes deposited in the Bertolani Collection (Department of Life Sciences, University of Modena and Reggio Emilia, Italy), 5 paratypes in the tardigrade slide collections of the Natural History Museum of Verona (Italy).

Type locality. sample C4322-Probe103, moss growing on tree bark, Black Forest, Germany, N 48° 32.135; E 8°12.948, 1058 m asl.

The new species *Ramazzottius kretschmanni* sp. nov. was found with *Milnesium* cf. *alpigenum*, *Macrobiotus hufelandi* group, *Isohypsibius prosostomus* Thulin, 1928, *Itaquascon* cf. *placophorum*, *Notahypsibius* cf. *pallidoides*, *Hypsibius scabropygus* Cuénot, 1929.

Etymology. The species is dedicated to Winfried Kretschmann, the political mastermind and founder of the Black Forest National Park.

Description. (morphometric data in Table I, Supplementary Tab. S2): Body colour is reddish. Eye spots are absent. Elliptical sensory structures are present on the head and visible with LM (Figures 1B, 3A,B). One small gibbosity is present on the external side of each leg of the fourth pair (Figures 1J, 3G), not clearly detectable in all specimens. Entire surface of the body is smooth without visible ornamentation with both LM and SEM (Figures 1L, 3A,B). With SEM, a "cheek-like" area is visible on each side of the head, at the level of the mouth opening (Figure 3C). It is an oval area slightly raised above the body surface that shows a different cuticular pattern (*i.e.* a net of very small meshes, < 0.1 μm; Figure 3E, F) compared with the rest of the body cuticle (Figure 3H). Within this "cheek-like" area there are: a dorsal region with several very small pores (more concentrated dorsally), a proximal cribrose area (for muscle attachment), and a ventral, almost rectangular, region with a few scattered, very small pores (Figure 3E).

Six peribuccal lobes are present around the antero-ventral mouth opening (Figures 1K, 3D). With SEM, small structures (called peribuccal papillae by Kaczmarek et al. 2006) are visible between the lobes (Figure 3D).

Feeding (bucco-pharyngeal) apparatus has a narrow buccal tube that is bent ventrally with slightly thicker walls located posteriorly to the stylet support insertion points (Figure 1C, D). The buccal armature, visible only with SEM (Figure 3D), is formed by a tiny anterior band of small teeth at the frontal extremity of the buccal tube (whose opening is rectangular in transverse section; Figure 3D) and a line of posterior teeth positioned in the anterior part of the buccal tube at the same level of the anterior part of the stylet sheaths (Figure 3D). With SEM, it was possible to observe only the four dorsal teeth in a line, but symmetrical ventral teeth could be present, as in *R. oberhaeuseri* (Stec et al. 2018). Apophyses for the insertion of the stylet

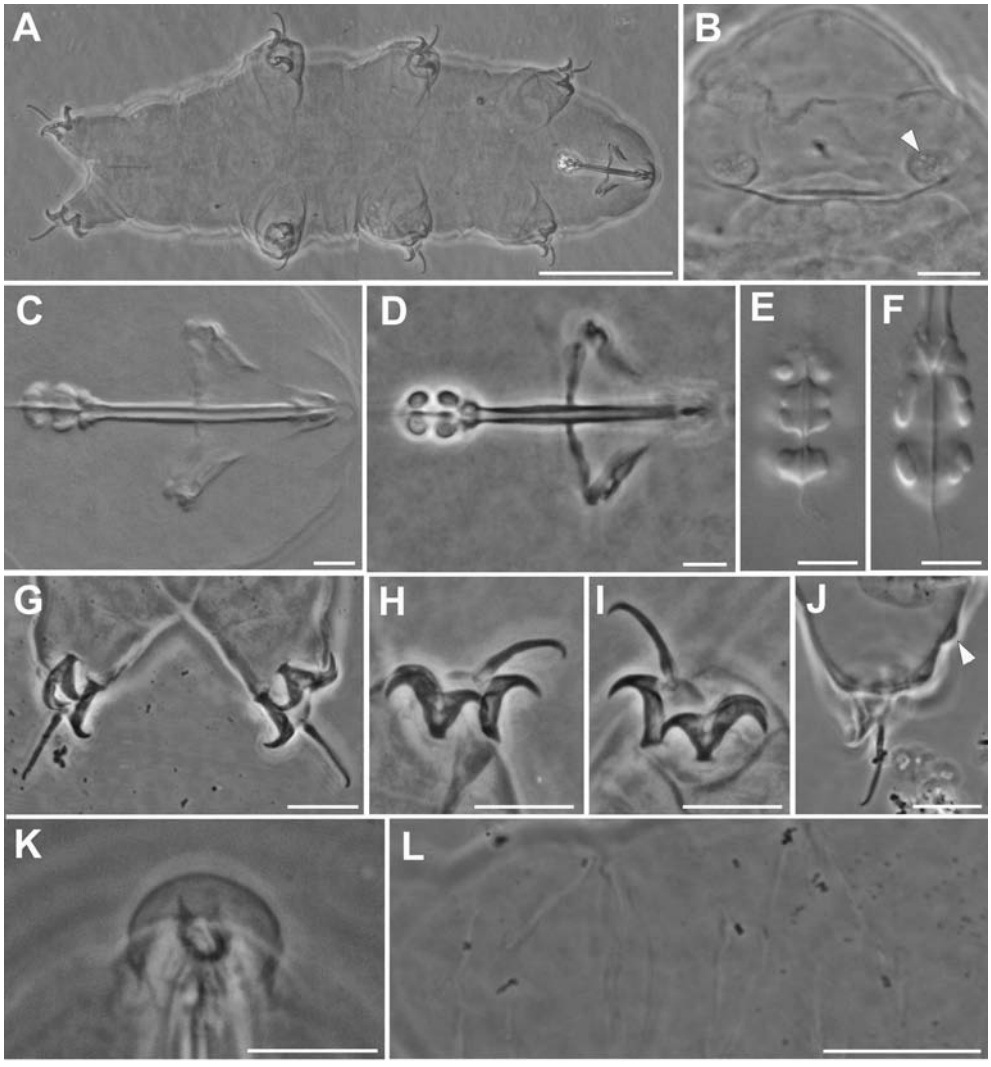

Figure 1. *Ramazzottius kretschmanni* sp. nov. (LM). A. In *toto* (ventral view). B. Elliptical organs on the head (arrowhead = pores). C-D. Feeding apparatus. D. Feeding apparatus (in focus the dorso-lateral macroplacoids). E. Macroplacoids (dorsal view). F. Macroplacoids (lateral view). G. Hind legs. H. Claws of II leg. I. Claws of III leg. J. Hind leg (arrowhead = gibbosity). K. Sensory area around mouth opening (COS). L. Posterior-dorsal cuticle. A, C, E, F, H, I, L: holotype. A, B, D, G-L: PhC. C, E, F: DIC. Scale bars: A, L = 50 μm; B-D, G-K = 10 μm; E, F = 5 μm.

muscles on the buccal tube are asymmetrical and with the typical shapes for the genus: dorsal apophysis is shorter and stumpy, with the caudal apex clearly prominent ("blunt hook") (Figure 1D); ventral apophysis has a less developed caudal apex. Stylet supports have an enlargement increasing from the proximal to the distal part (Figure 1D). Each stylet furca has two wide spherical condyles laterally flattened and internally sclerified, supported by short branches with large apophyses. Pharynx has large triangular apophyses and two macroplacoids (the first is clearly longer than the second in larger specimens; Figure 1C -F). The shape and size of the placoids can change slightly between specimens. When the placoids are observed in lateral view (Figure 1F), the first macroplacoid is grain-shaped (sub-spherical in smaller specimens; Figure 1D), while the second is sub-spherical; in dorsal view (Figure 1E), the first macroplacoid is drop-shaped (a small median incision is visible in some specimens), while the second is rectangular with rounded corners and without incision.

Claws are of the *Ramazzottius* type (*oberhaeuseri* variant; according to Guidetti et al. 2019b) and moderately sized (Figure 1G -I, 3F-G). Claws of the same leg are extremely different from one another in size and shape (Table I). The main (primary) branch of the external claws is straight and curved only distally, with small accessory points (difficult to see with LM) that run parallel and

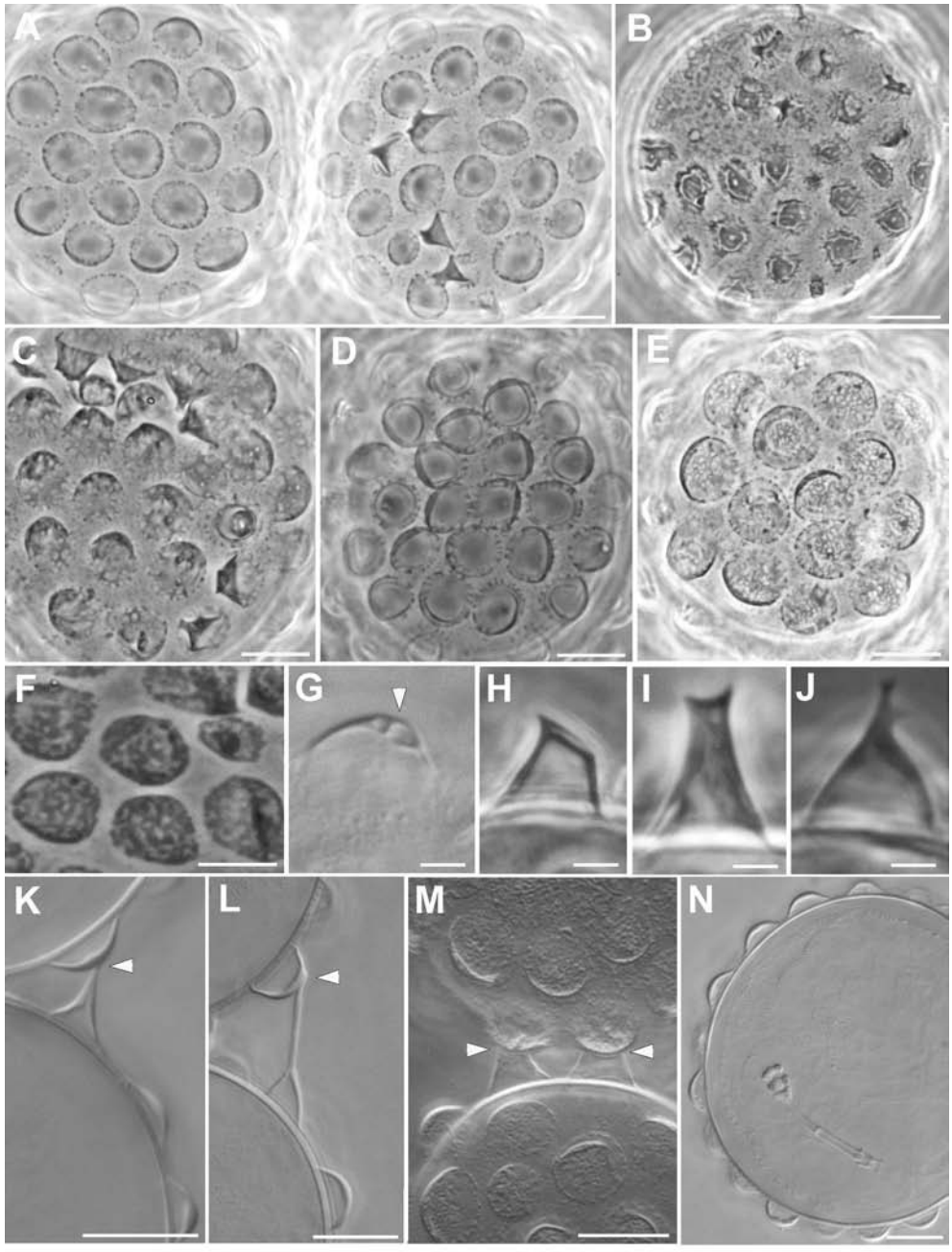

Figure 2. *Ramazzottius kretschmanni* sp. nov. (LM). A. Two eggs with the most common morphology. B. Egg considered aberrant. C-E. Egg. F. Egg process with "bubble-like" empty spaces within the distal wall (arrowhead). G. Egg processes considered aberrant. H-J. Abnormal egg process. K-M. Contact between two processes of different eggs (arrowhead). N. Egg with a developing embryo. A-E, G-J: PhC. F, K-N: DIC. Scale bars: A-F, K-N = 10 μm; G-J = 2 μm.

coplanar to the branch (Figures 1I, 3G). The primary branch is connected by a couple of thin cuticular filaments to the basal portion of the claw (that is continuous with the secondary branch) forming a non-sclerotized portion of the branch (the light refracting unit, LRU; Figure 1G -I). Length of branches increase slightly from the first to the fourth legs. The secondary branch of external claws is short and stumpy; it is inserted on a short basal portion and has evident accessory points (Figure 1G -I, 3F-G). Pseudolunules are visible in the hind claws, although thin and barely visible; in the external claws they are extended towards the internal leg.

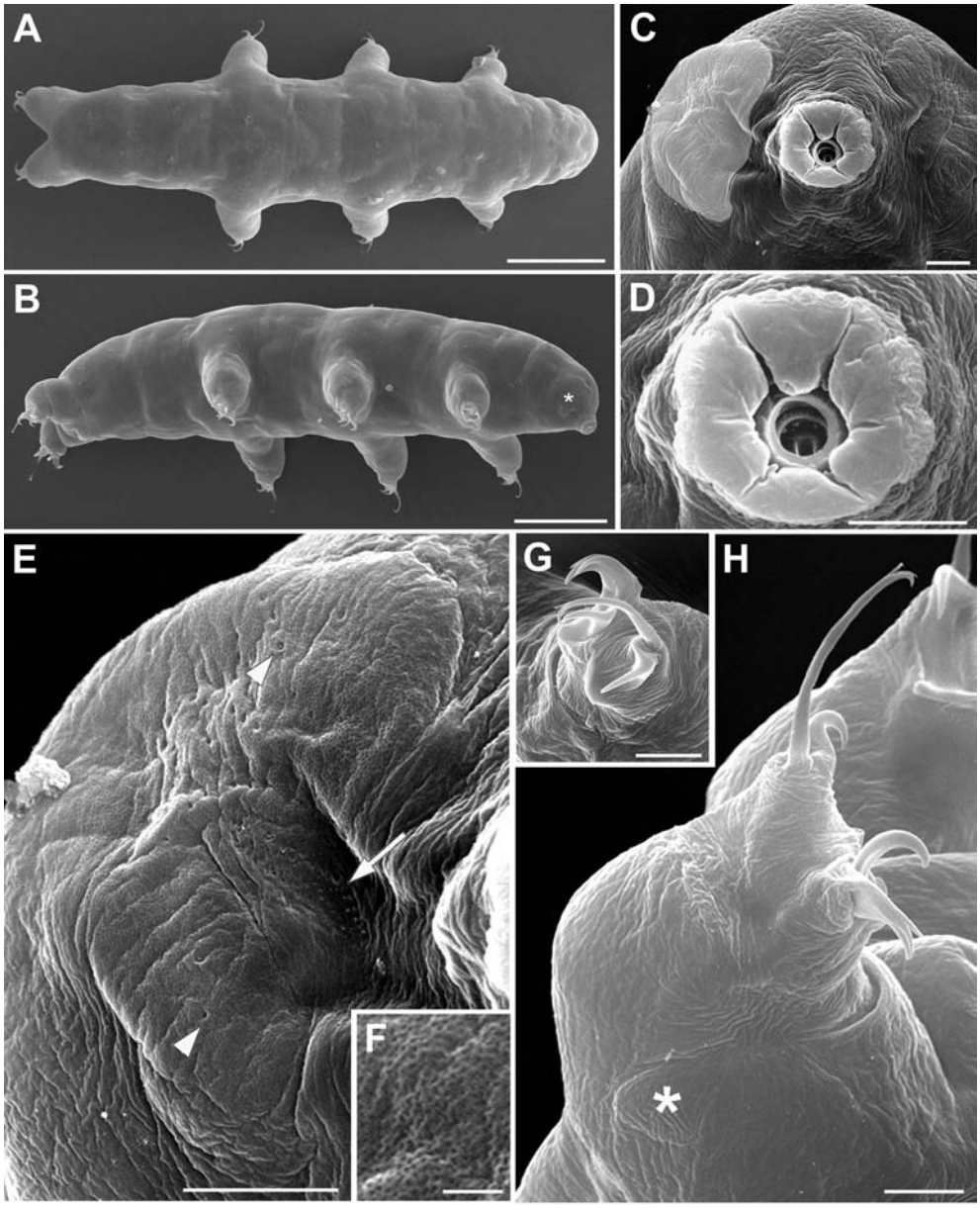

Figure 3. *Ramazzottius kretschmanni* sp. nov. (SEM). A. In *toto* (dorsal view). B. In *toto* (ventro-lateral view), asterisk = "cheek-like" area. C. Head (frontal view), lighter color indicates one "cheek-like" area. D. Mouth opening (magnification of C). E. "Cheek-like" area in the head (magnification of C), arrowheads = pores, arrow = cribrose area. F. Surface of the "cheek-like" area with a net of very small meshes. G. Claws of II leg. H. Hind leg, asterisk = gibbosity. Scale bars: A-B = 50 μm; C-E, G-H =5 μm; F = 1 μm.

Eggs are laid freely in the environment and have an ornamented shell (Figures 2, 4A,B). Eggs are circular or slightly oval, with a diameter without processes of 49.1–66.9 μm (mean 56.5 μm, SD 5.0 μm; N = 15). Egg shell has hemispherical processes (the size and appearance of which can vary between eggs; Figure 2 A-F), interspersed with few processes of irregular shape (e.g. resembling cones and truncated cones; Figure 2H -J, 4A). The heights and diameters of the hemispherical processes can vary between eggs (height: mean 3.8 μm, SD 0.5 μm, min 2.7 μm, max 4.8 μm; diameter: mean 7.9 μm, SD 1.3, min 4.6 μm, max 11.5 μm; N = 54 from 10 eggs). The process heights are generally lower or similar to half of the process diameters, with a mean percentage (ratio diameter/height) of 211.7% (SD 35.7; min 135.4, max 303.6; N = 54 from 10 eggs); two eggs, considered aberrant, show very flat processes (not measurable) with irregular margins (Figure 2B, F). The thickness of the wall of the egg processes increases distally (Figure 2G, K); in several eggs,

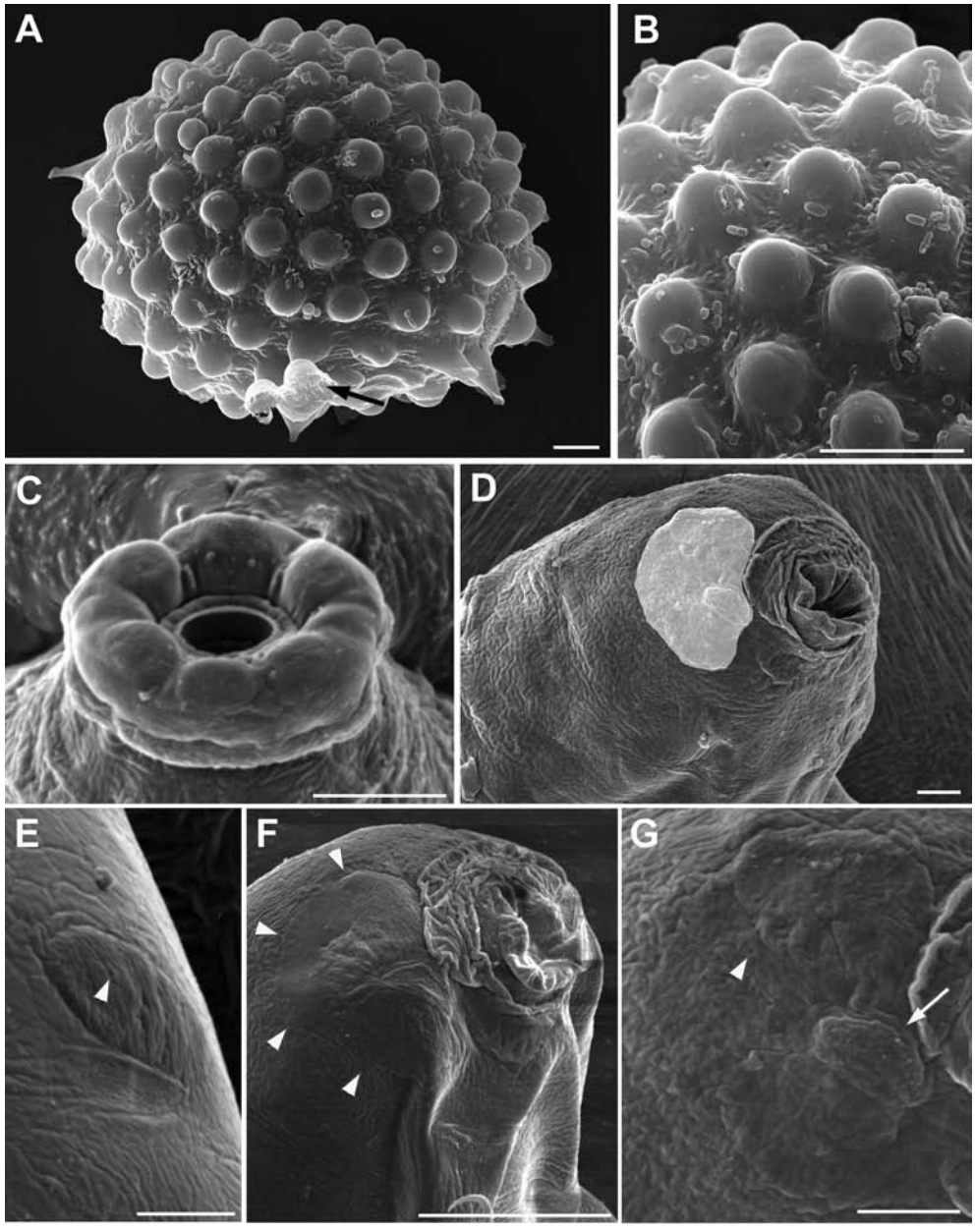

Figure 4. *Ramazzottius kretschmanni* sp. nov. (A-B) and *Cryoconicus antiarkctos* (C-G) (SEM). A. Egg, arrow = irregular indented margin of a broken egg process. B. Egg surface. C. Mouth opening (with COS). D. Head (frontal-lateral view), lighter color indicates the "cheek-like" area (ALS). E. Elliptical organ on the head (PLS), arrowhead = pore. F. Head (lateral view), arrowheads indicate the "cheek-like" area. G. "Cheek-like" area (magnification of B), arrowhead = pore, arrow = cribrose area. Scale bars = 5 μm.

within the process wall, empty "bubble-like" spaces can be present (Figure 2G), leading to an irregular appearance of the process surface with LM (Figure 2C, E-F). There are about 15–22 processes (mean 18.2, SD 2.1; N = 15) on the egg circumference and on an egg surface of 1000 μm^2 is possible to count from 9 to 18 processes (mean 11.9, SD 2.4; N = 15). Surface of the processes is smooth. The base of the processes is round with an irregular indented margin visible only with LM (Figure 2A -E); in some eggs, the indentations of the margin can be very long and evident (Figure 2D). This indented margin develops below the shell surface (internally) and is visible with SEM only in broken processes (Figure 4A). Egg shell surface between processes is generally smooth (Figure 2A), but some eggs show dots with LM (Figure 2C, E) and small irregular crests with SEM (Figure 4B). Most eggs were found in pairs within the sample; each pair was kept together

Table I. Morphometric data and Thorpe's Normalization analysis for the animals of *Ramazzottius kretschmanni* sp. nov. In grey the p value below 0.05 indicates the structures that have an allometric growth. Allometric exponent (b) and the Y intercept (a*) of the regression of Thorpe normalized traits are presented.

		RANGE						MEAN		SD		Holotype		Thorpe's Normalization		
CHARACTER	N		µm			pt		µm	pt	µm	pt	µm	pt	b	a*	p_value
Body length	21	213	–	357	*820*	–	*1344*	278	*1005*	39	*124*	213	*829*	*1.2614*	*204.2312*	*0.1223*
Buccopharyngeal tube																
Buccal tube length	21	25.7	–	31.5		–		27.6	–	1.6	–	25.7	–	*1.0000*	*0.0000*	
Stylet support insertion point	21	14.5	–	17.6	*54.2*	–	*61.2*	15.7	*57.0*	0.8	*1.7*	14.5	*56.6*	*0.8882*	*0.7264*	*0.7285*
Buccal tube external width	21	1.8	–	2.3	*6.3*	–	*8.0*	2.0	*7.2*	0.1	*0.4*	2.0	*7.6*	*0.6648*		*0.0025*
Buccal tube internal width	21	0.7	–	1.0	*2.5*	–	*3.5*	0.8	*2.9*	0.1	*0.2*	0.7	*2.8*	*0.9578*	*0.2253*	*0.7362*
Placoid lengths																
Macroplacoid 1	21	2.4	–	3.5	*8.2*	–	*12.6*	2.9	*10.4*	0.3	*1.1*	2.9	*11.4*	*1.2858*	*−0.8787*	*0.1032*
Macroplacoid 2	21	2.2	–	2.8	*7.5*	–	*9.7*	2.5	*8.9*	0.2	*0.5*	2.3	*9.0*	*0.7720*	*0.1699*	*0.1026*
Macroplacoid row	21	5.6	–	7.1	*17.9*	–	*24.2*	6.1	*22.3*	0.5	*1.5*	5.8	*22.7*	*1.1763*	*−1.0806*	*0.5236*
mac2/mac1		69.3	–	98.8	*69.3*	–	*98.8*	86.5	*86.5*	7.9	*7.9*					
Claw 1 heights																
External base	17	6.1	–	8.2	*22.0*	–	*31.3*	7.0	*25.3*	0.8	*2.5*	6.1	*23.8*	*1.6321*	*−5.6625*	*0.1379*
External primary branch	18	7.7	–	11.5	*27.9*	–	*43.9*	9.2	*33.4*	1.2	*4.1*	7.7	*30.0*	*0.8081*	*4.1764*	*0.0341*
External secondary branch	15	4.6	–	6.5	*16.8*	–	*24.6*	5.4	*19.5*	0.5	*2.2*	4.8	*18.7*	*1.2706*	*−1.4825*	*0.2947*
Internal base	21	4.1	–	6.7	*14.9*	–	*25.4*	5.2	*18.8*	0.9	*2.8*	4.4	*17.2*	*1.2787*	*0.8526*	*0.0378*
Internal primary branch	12	5.6	–	6.9	*19.9*	–	*26.4*	6.2	*22.1*	0.5	*1.8*	5.6	*21.8*	*0.3235*	*5.4104*	*0.0000*
Internal secondary branch	19	4.2	–	6.6	*15.3*	–	*25.2*	5.2	*18.9*	0.7	*2.5*	4.5	*?*	*1.1555*	*1.1693*	*0.2901*
Claw 2–3 heights																
External base	19	6.5	–	9.3	*24.6*	–	*34.3*	7.6	*27.5*	0.9	*2.6*	6.5	*25.3*	*1.5066*	*−2.1107*	*0.1698*
External primary branch	21	8.1	–	12.4	*31.7*	–	*47.1*	10.3	*37.3*	1.2	*3.6*	8.1	*31.7*	*1.3964*	*−0.9013*	*0.1052*
External secondary branch	18	4.7	–	7.1	*17.4*	–	*27.0*	5.9	*21.4*	0.6	*2.1*	5.3	*20.4*	*1.0153*	*1.5578*	*0.9227*
Internal base	21	4.2	–	6.7	*15.3*	–	*25.2*	5.4	*19.6*	0.8	*2.4*	4.7	*18.2*	*1.3164*	*0.6272*	*0.0600*
Internal primary branch	18	6.0	–	8.4	*21.4*	–	*31.8*	6.8	*24.4*	0.8	*2.6*	6.1	*23.7*	*0.3452*	*4.8584*	*0.0000*
Internal secondary branch	21	4.5	–	6.8	*16.8*	–	*26.0*	5.5	*20.1*	0.7	*2.3*	4.7	*18.2*	*1.2766*	*0.1762*	*0.1264*
Claw 4 lengths																
Anterior base	17	4.4	–	7.1	*16.5*	–	*26.7*	5.5	*20.0*	0.8	*2.7*	4.7	*18.4*	*0.8914*	*2.5500*	*0.2725*
Anterior primary branch	15	6.0	–	8.7	*22.2*	–	*31.3*	7.0	*25.1*	0.8	*2.4*	6.0	*23.3*	*0.9444*	*0.8679*	*0.7876*
Anterior secondary branch	19	4.6	–	7.1	*16.8*	–	*27.1*	5.8	*20.8*	0.8	*2.7*	4.7	*18.2*	*1.3613*	*0.3510*	*0.0753*
Posterior base	16	6.9	–	9.3	*25.1*	–	*35.2*	8.0	*29.0*	0.9	*2.9*	6.9	*27.0*	*1.4417*	*−2.5275*	*0.1642*
Posterior primary branch	19	10.7	–	16.2	*41.5*	–	*61.5*	12.7	*45.9*	1.3	*4.7*	10.7	*41.5*	*0.7508*	*5.6243*	*0.0140*
Posterior secondary branch	13	4.8	–	7.4	*15.7*	–	*26.6*	5.9	*21.1*	0.8	*3.0*	5.0	*19.5*	*0.9443*	*0.2652*	*0.6684*

by connections between conical shaped processes and hemispherical processes (Figure 2K -M). Three eggs with a fully developed embryo were found (Figure 2N).

Morphological differential diagnosis

Ramazzottius kretschmanni sp. nov. is characterized by smooth cuticle, "cheek-like" area (described above), and egg shell with two types of processes (i.e. most hemispherical and some conical/truncoconical).

Based on the claw morphology, Guidetti et al. (2019b) identified two groups of species within the genus *Ramazzottius*: the "*oberhaeuseri* group" characterized by claws of *Ramazzottius* type with *oberhaeuseri* variant (main branch connected to the secondary branch by two thin cuticular filaments, forming an LRU), and the "*nivalis* group" characterized by claws of the *cataphractus* variant (main branch detached from secondary branch). Based on egg morphology, Stec et al. (2018) identified the "*oberhaeuseri* complex" characterized by species with hemispherical egg processes. Accordingly, the new species, *R. kretschmanni* sp. nov., belongs to the "*oberhaeuseri* complex" based on egg morphology and to the "*oberhaeuseri* group" based on claw morphology. Within this group of species, the claw morphology is generally constant with differences among species only related to morphometric traits.

Ramazzottius kretschmanni sp. nov. differs from all the other species of the genus that have smooth cuticle or very weak dorsal posterior cuticular ornamentation. In particular, it differs from:

Ramazzottius andreevi Biserov 1997/98 by having a completely smooth cuticle in all specimens (in *R. andreveei* the cuticle sculpture is poorly developed, completely smooth only in some specimens; Figure 5N) and shape of the egg processes (small and thin cones in *R. andreveei*; Figure 5P);

Ramazzottius anomalus (Ramazzotti, 1962a) by the shape of the egg processes (long cone/aculeus in *R. anomalus*; Figure 6G), and egg surface smooth or with small dots (large granules in *R. anomalus*; Figure 6F);

Ramazzottius caucasicus Biserov, 1997/98 by the shape of the egg processes (long cones with enlarged base in *R. caucasicus*; Figure 6K) and egg surface smooth or with small dots (smooth with scarcely distributed pores in *R. caucasicus*; Figure 6K);

Ramazzottius montivagus (Dastych, 1983) by more slender main branch of external claws, with smaller accessory points, in the first three pair of legs (e.g. compare Figs. 5-7 in Dastych 1983 to Figure 1 H,J). Morphometric comparisons are difficult due to the absence of clear morphometric data for *R. montivagus*. The egg of *R. montivagus* are unknown;

Ramazzottius oberhaeuseri (Doyère, 1840) (following the redescription by Stec et al. 2018) by evident elliptical organs on the head (poorly visible in *R. oberhaeuseri*), smooth cuticle (both with LM and SEM; *R. oberhaeuseri* shows a weak posterior polygonal sculpture), lower height of the egg processes (4.6–8.6 µm, mean 6.6 µm in *R. oberhaeuseri*), and higher percentage ratio of process diameter/height (97–197%, mean 141% in *R. oberhaeuseri*);

Ramazzottius semisculptus Pilato & Rebecchi, 1992 (Figure 7) by completely smooth cuticle (a weak posterior polygonal sculpture can be present in *R. semisculptus*), shorter placoid row (*pt* 26.5–30.8 in *R. semisculptus*) and shape of the egg processes (conical in *R. semisculptus*);

Ramazzottius subanomalus Biserov, 1985 by shape of the egg processes (conical in *R. subanomalus*; Figure 8D);

Ramazzottius valaamis Biserov & Tumanov, 1993 by the shape of the egg processes (filamentous in *R. valaamis*; Figure 9F). A net-like sculpture, previously undescribed, was found on the cuticle of a paratype of *R. valaamis* (Figure 9I), but is absent in the new species.

Ramazzottius kretschmanni sp. nov. differs from the other species of the genus that have hemispherical egg processes [*i.e. R. affinis, Ramazzottius libycus* Pilato, D'Urso & Lisi, 2013, *R. oberhaeuseri, R. thulini*] by the presence of smooth cuticle as all the other species have ornamented cuticle with hemispherical tubercles with a polygonal base. The cuticle of *R. oberhaeuseri* appears weakly ornamented with LM only in freshly mounted specimens or with SEM observations (Stec et al. 2018). The eggs of *R. kretschmanni* sp. nov. differ from those of *R. affinis* (Figure 5 G,H) by the more regular shape of the processes (i.e. only few processes are not emispherical).

Molecular characterization

It was possible to amplify *cox1* sequences from four specimens of *R. kretschmanni* sp. nov. (C4322 T1-T4), obtaining sequences of 549 bp, representing three different haplotypes with a p-distance of 0.2–0.4% (Figure 10; Tab. S1). The most similar haplotype (p-distance: 17.2%) to another species belongs to a population of *Ramazzottius* from Denmark (Tab. S1). The other available haplotypes from GenBank have p-distances ranging from 17.7% to 22.4% (Tab. S1) compared to that of *R. kretschmanni* sp. nov.

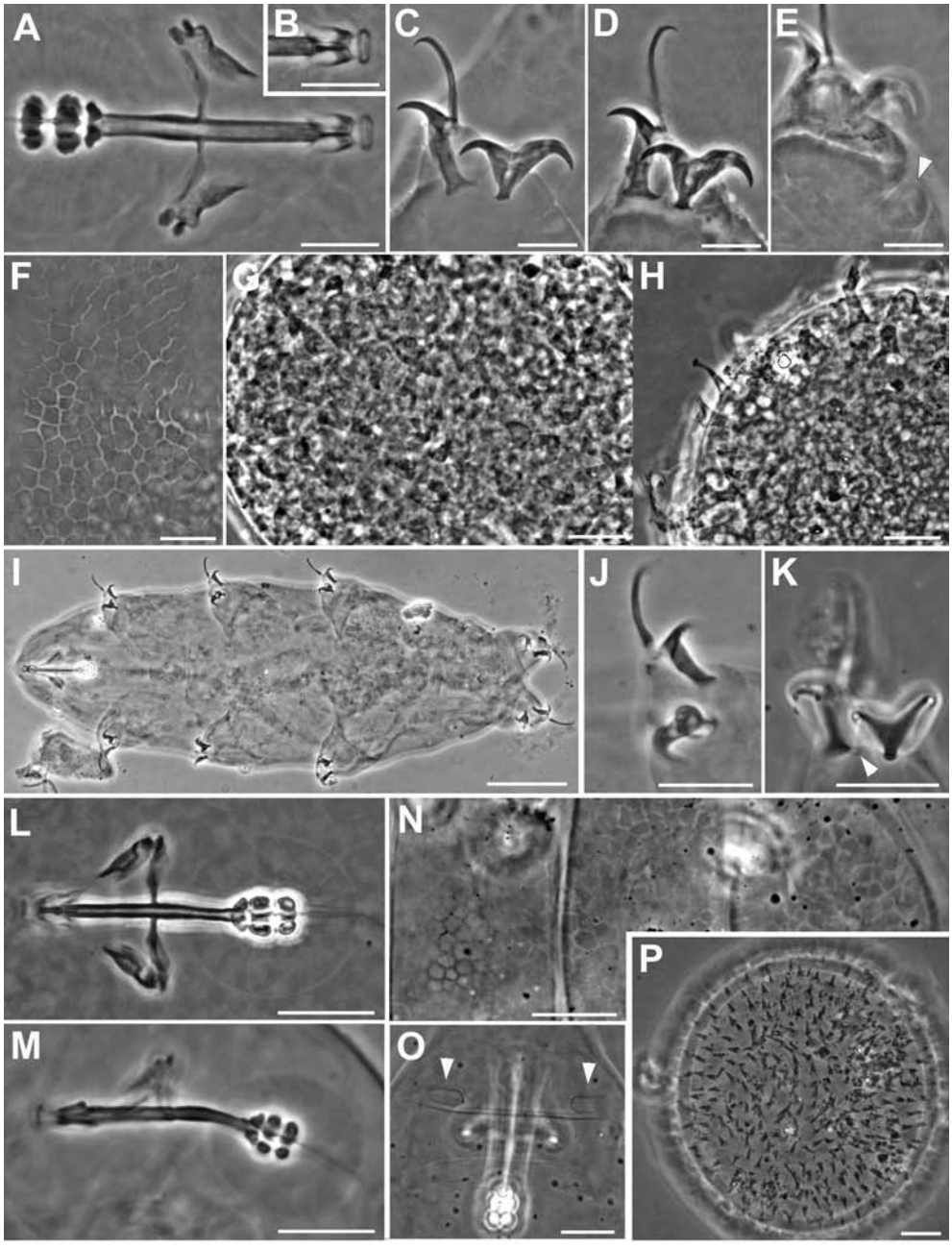

Figure 5. *Ramazzottius affinis* (A-H) and *Ramazzottius andreevi* (I-P) (LM, PhC). A. Feeding apparatus (ventral view). B. Apophysis for the insertion of the stylet muscles (dorsal view). C. Claws of II leg. D. Claws of IV leg. E. Hind leg (arrowhead = small papilla). F. Posterior-dorsal cuticle. G-H. Egg surface at two levels of focus. I. Animal in *toto*. J. Claws of II leg. K. Claws of IV leg, arrowhead = pseudolunule. L. Feeding apparatus (dorsal view). M. Feeding apparatus (lateral view). N. Posterior-dorsal cuticle. O. Elliptical organs on the head (arrowheads). P. Egg surface. A-E, I-J: holotype. Scale bars: A-H, J-P = 10 μm; I = 50 μm.

It was also possible to amplify ITS2 sequences of the same four specimens (C4322 T1-T4), obtaining sequences of 501 bp, representing four different haplotypes with a p-distance of 0.2–1.9% (Figure 11; Tab. S1). The most similar haplotype (p-distance: 2.3%) belongs to a population of *Ramazzottius* from Austria (Tab. S1). The other available haplotypes from GenBank have p-distances ranging from 3.1% to 21.6% (Tab. S1). In the comparison with *R. oberhaeuseri* (the type species of the genus), *R. kretschmanni* sp. nov. has p-distances of 18.9–19.1% for the *cox1* sequences and 13.3–14.0% for the ITS2 sequences.

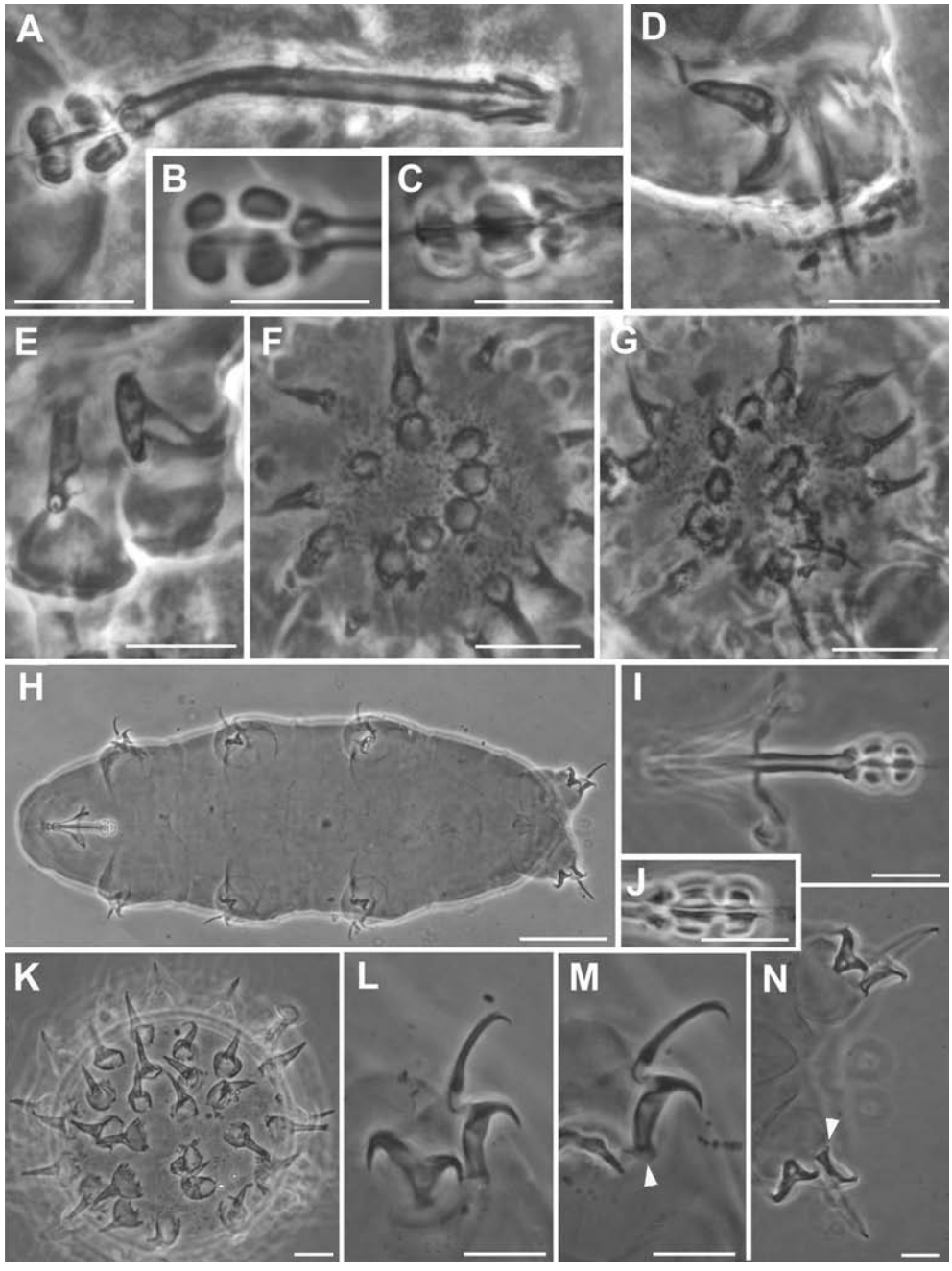

Figure 6. *Ramazzottius anomalus* (A-G) and *Ramazzottius caucasicus* (H-N) (LM, PhC). A. Feeding apparatus (lateral view). B. Macroplacoids (lateral view). C. Macroplacoids (dorsal view). D. Claws of III leg. E. Claws of IV leg. F-G. Egg surface at two levels of focus. H. Animal in *toto*. I. Feeding apparatus. J. Macroplacoids (dorsal view). K. Egg surface. L. Claws of II leg. M. Claws of III leg, arrowhead = pseudolunule. N. Hind legs, arrowhead = pseudolunule. A-G: Syntype. H, I, L-N: holotype. Scale bars: A-G, I-N = 10 μm; H = 50 μm.

The PTP analysis for the *cox1* gene (Figure 10, left) shows 13 putative species clusters, with *R. kretschmanni* sp. nov. in basal position and clearly separated from all other putative *Ramazzottius* species. The validity of *R. kretschmanni* sp. nov. is further confirmed by both the ASAP and the haplotype network analysis (Figure 10, centre and right) for the *cox1* gene. The PTP analysis for the ITS2 gene (Figure 11, left) shows five clusters, again with *R. kretschmanni* sp. nov. clearly separated from all other putative *Ramazzottius* species.

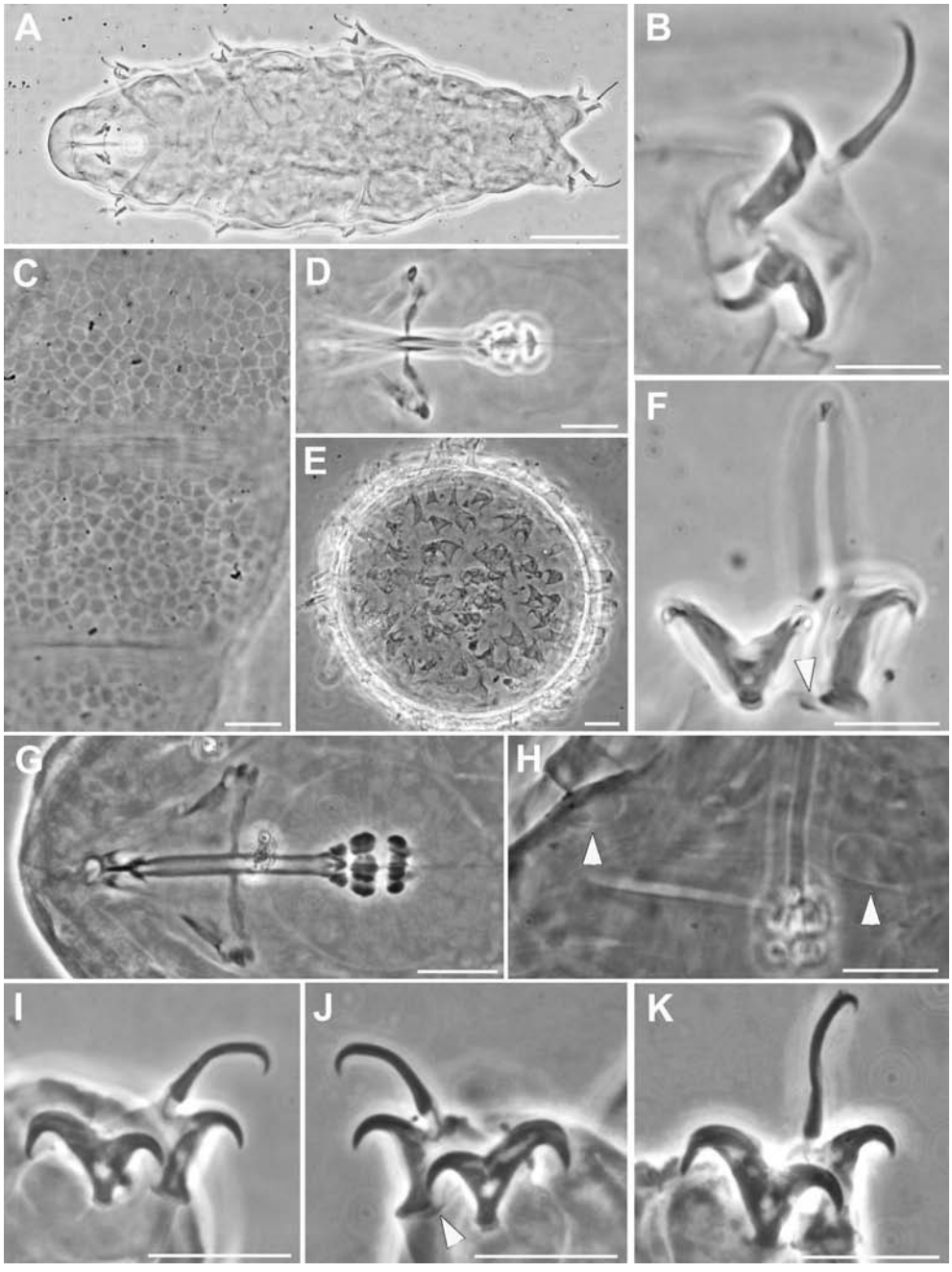

Figure 7. *Ramazzottius rupeus* (A-F) and *Ramazzottius semisculptus* (G-K) (LM, PhC). A. Animal in toto. B. Claws of II leg. C. Posterior-dorsal cuticle. D. Feeding apparatus. E. Egg surface. F. Claws of IV leg, arrowhead = pseudolunule. G. Feeding apparatus. H. Elliptical organs on the head (arrowheads). I. Claws of II leg. J. Claws of II leg, arrowhead = pseudolunule. K. Claws of IV leg. A, C, D, F: holotype. Scale bars: A = 50 μm; B-K = 10 μm.

The validity of *R. kretschmanni* sp. nov. is further confirmed by the ASAP analysis of ITS2 gene (Figure 11, centre), whereas the haplotype network analysis (Figure 11, right) shows a further partition inside the German population, flagging specimen C4322 T2 as belonging to a different partition with respect of the other analysed specimens.

Observations and taxonomic considerations on *Ramazzottius* species

Ramazzottius affinis (**Figure 5A-H**)

The original description (Bertolani et al. 1994) provided only drawings of the species. Being the species description in Italian, we report the description of

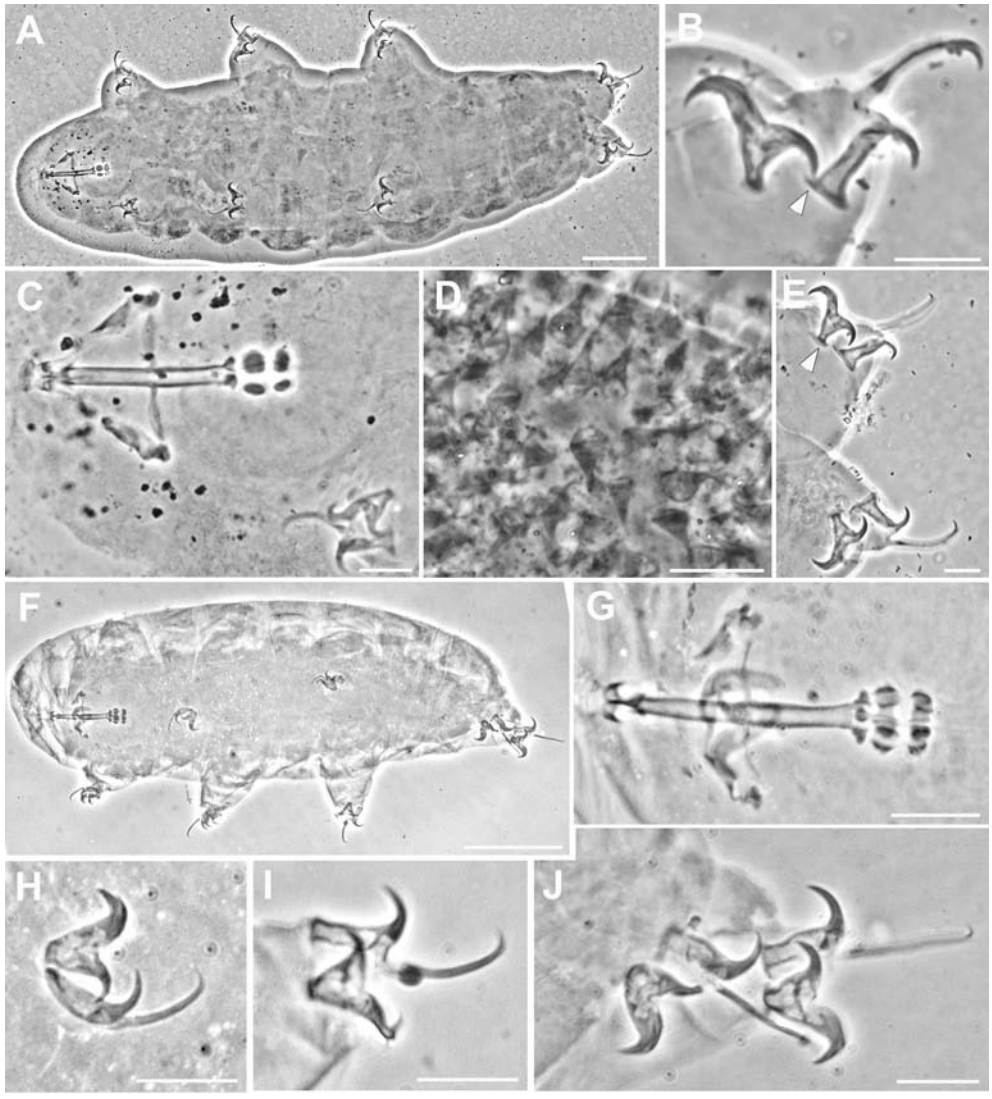

Figure 8. *Ramazzottius subanomalus* (A-E) and *Ramazzottius thulini* (F-J) (LM, PhC). A. Animal in toto. B. Claws of II leg, arrowhead = pseudolunule. C. Feeding apparatus. D. Egg surface. E. Claws of IV leg, arrowhead = pseudolunule. F. Animal in toto. G. Feeding apparatus. H. Claws of II leg. I. Claws of III leg. J. Claws of IV leg. A-C, E-J: holotype. Scale bars: A, F = 50 μm; B-E, G-J = 10 μm.

the main characters of the species as reported by Bertolani et al. (1994) and confirmed by our observations (for morphometric data see Bertolani et al. 1994). Eye spots are absent. Sculptured dorsal cuticle with 5–6 bands of small hemispherical tubercles (diameter 2.7–3.8 μm; Figure 5F), on the posterior two-thirds of the animal, alternated with thin smooth bands; the sculpture results absent in the anterior one-third or sometime in the first half of the animal.

Two evident elliptical organs present on the head. A small papilla (not cited in the original description) presents on the external side of each leg on the fourth pair (in the holotype; Figure 5E). Transversal bands of epidermal cells with brown-reddish pigments (posteriorly corresponding to the bands of tubercles of the cuticle) alternated with not pigmented bands are present. Buccal ring without lamellae but, dorsally and ventrally, with a line of six very tiny teeth. Apophyses for the insertion of the stylets muscles (AISM) are asymmetrical respect to the frontal plane in shape of blunt hooks (dorsal crest thicker than the ventral; Figure 5A,B). Buccal tube with thicker walls after the stylet support insertion (not cited in the original description; Figure 5A). Pharyngeal bulb with evident apophyses, more developed transversally, and two granular macroplacoids (the first with a small indentation in the middle and the largest). Long claws of the *Ramazzottius* type, *oberhaeuseri* variant

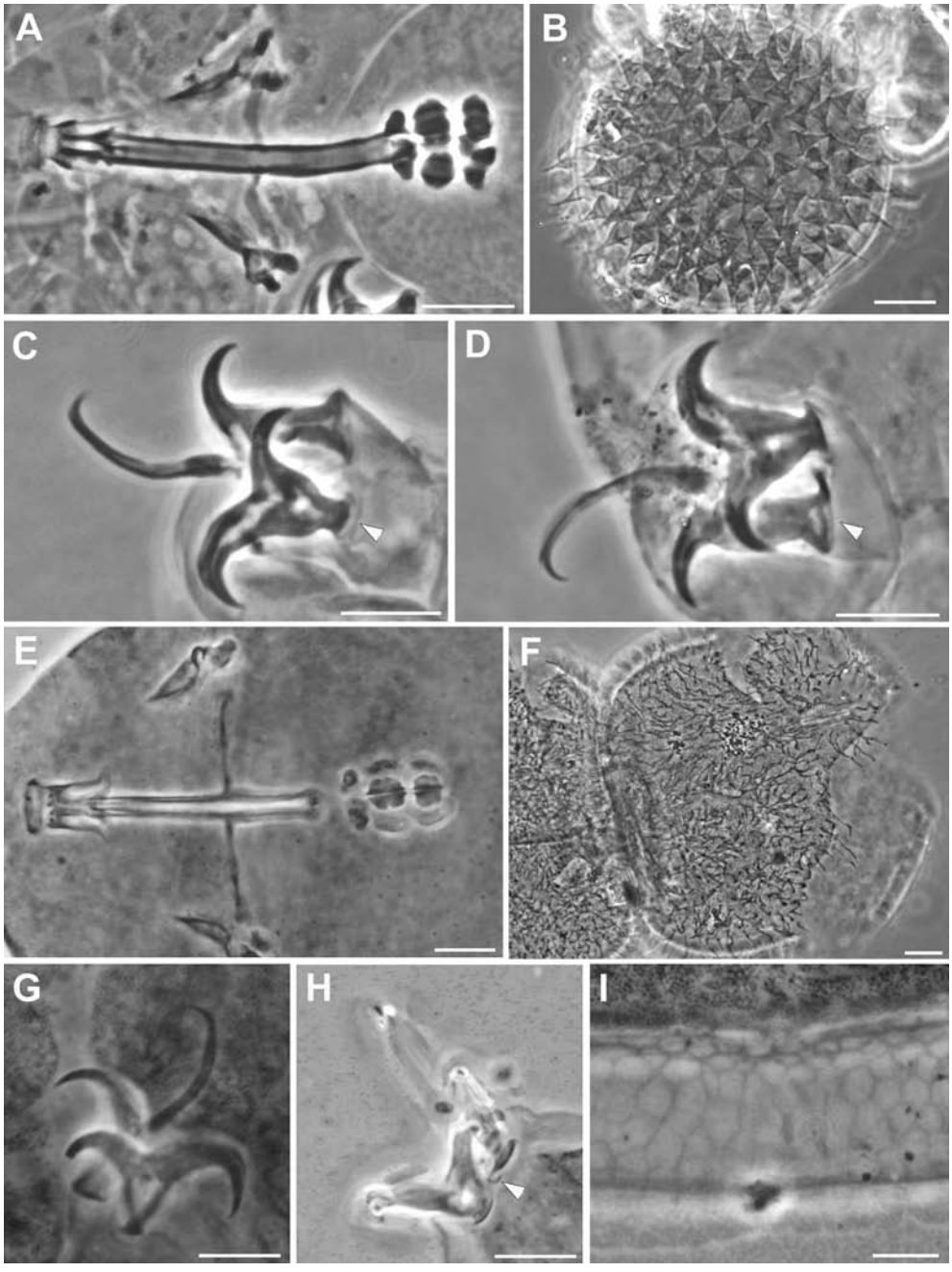

Figure 9. *Ramazzottius tribulosus* (A-D) and *Ramazzottius valaamis* (E-I) (LM, PhC). A. Feeding apparatus. B. Egg surface. C. Claws of I leg, arrowhead = pseudolunule. D. Claws of IV leg, arrowhead = pseudolunule. E. Feeding apparatus. F. Egg surface. G. Claws of II leg. H. Claws of IV leg, arrowhead = pseudolunule. I. Dorsal cuticle surface. A, C-E, G-H: holotype. Scale bars = 10 μm.

(according to Guidetti et al. 2019b), with not very evident accessory points, especially in the external claws, and with thin pseudolunula (Figure 5C,D). Eggs are free laid and ornamented with two type of processes: conical processes with relatively large base, the most abundant, and truncated-cone processes (Figure 5G,H).

Ramazzottius andreevi **(Figure 5I-P)**

The original description (Biserov 1997/98) provided only drawings of the species, we provide LM pictures of all the taxonomic characters considered in the description of the species. The characters of the type specimens examined correspond to the original description. Based on our obeservations, the following

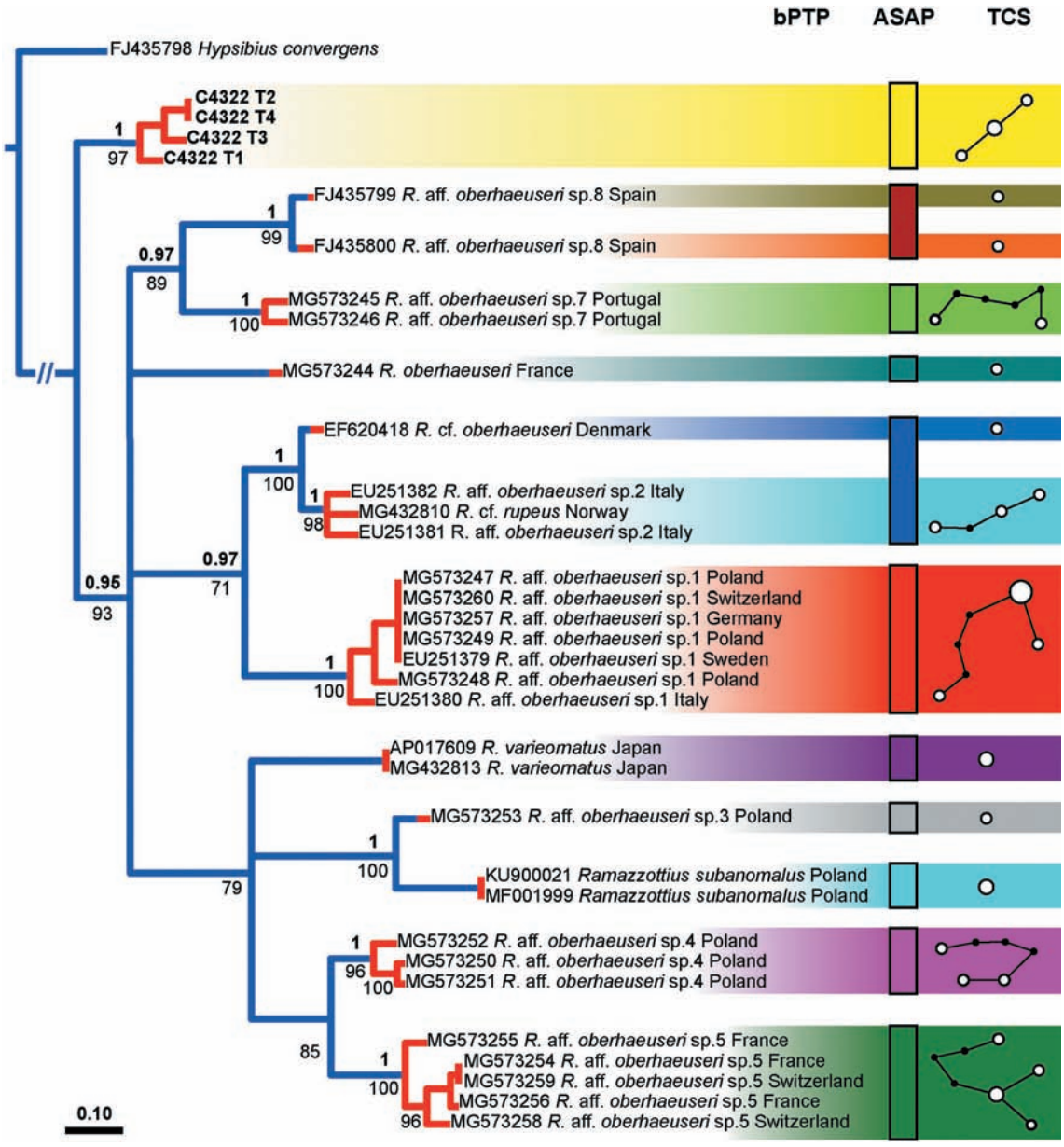

Figure 10. Left: tree resulting from both the Bayesian inference and the maximum likelihood analysis of *cox1* in *Ramazzottius kretschmanni* sp. nov. specimens and sequences from GenBank of *Ramazzottius* species. Values above branches denote posterior probability values, while values under branches represent bootstrap values. Results of the Poisson tree process analysis are provided using differently coloured branches: putative species are indicated using transitions from blue-coloured branches to red-coloured branches. Newly scored haplotypes are in bold. The scale bar shows the number of substitutions per nucleotide position. Centre: rectangles denote specimens grouped by ASAP analysis (asap-score: 3.00). Right: haplotype network analysis. Circles represent haplotypes, while circle surface denotes haplotype frequency. Networks falling below the value of the 95% connection limit are disconnected.

characters can be added to the original description as: the presence of clearly visible cuticular sculpture, with polygonal flat tubercles (Figure 5N) and visible elliptical organs on the head (Figure 5O) (according to Biserov (1997/98) both characters are inconspicuous and/or not visible); an increase of the thickness of the buccal tube wall after the stylet support insertion point (Figure 5L,M); a light refracting unit (LRU) in the main branch of external claw on all legs (Figure 5J).

Ramazzottius anomalus (Figure 6A-G)

The original description (Ramazzotti 1962a) provided only drawings of the species, we provide LM

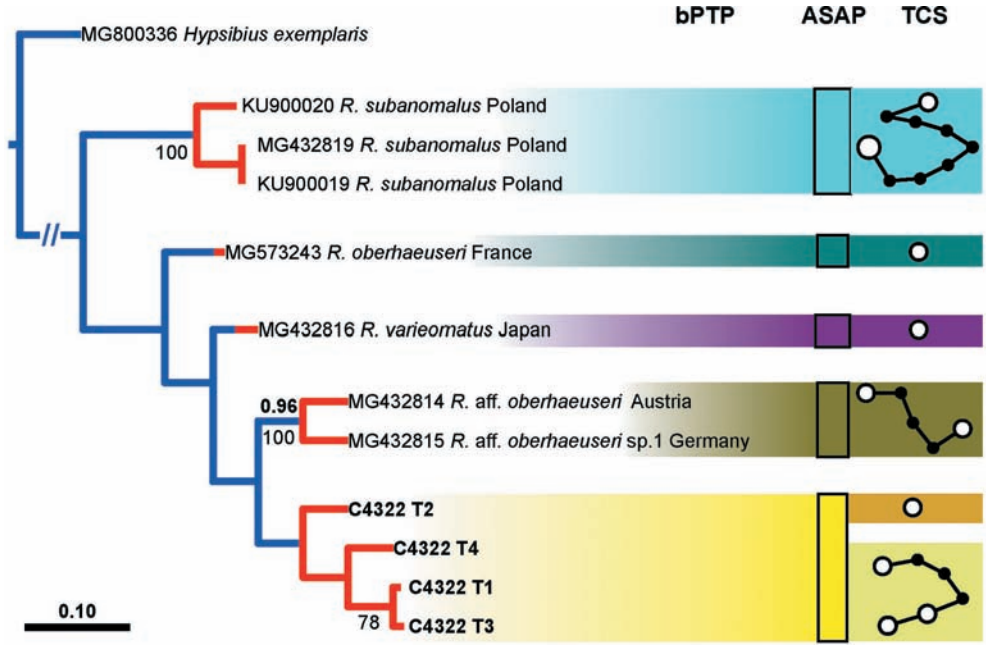

Figure 11. Left: tree resulting from both the Bayesian inference and the maximum likelihood analysis of ITS2 in *Ramazzottius kretschmanni* sp. nov. specimens and sequences from GenBank. Values above branches denote posterior probability values, while values under branches represent bootstrap values. Results of the Poisson tree process analysis are provided using differently coloured branches: putative species are indicated using transitions from blue-coloured branches to red-coloured branches. Newly scored haplotypes are in bold. The scale bar shows the number of substitutions per nucleotide position. Centre: rectangles denote specimens grouped by ASAP analysis (asap-score: 1.50). Right: haplotype network analysis. Circles represent haplotypes, while circle surface denotes haplotype frequency. Networks falling below the value of the 95% connection limit are disconnected.

photographs of the bucco-pharyngeal apparatus, claws and eggs of the species. Some photographs of the type series were published in Stec et al. (2017). We report photographs of the dorsal and ventral crests of the AIMS in lateral view (Figure 6A) never represented before. The characters of the type specimen examined correspond to the original description. To avoid future misunderstanding, we specify that the original description of the species is not in Ramazzotti (1962b), as reported by some authors (e.g. Kaczmarek et al. 2015; Stec et al. 2017), but in Ramazzotti (1962a).

Ramazzottius caucasicus (Figure 6H-N)

The original description (Biserov 1997/98) provided drawings of the species and four SEM pictures of a claw, the cuticle and eggs, we provide LM photographs of all the taxonomic characters considered in the description of the species, including the pseudolunules in the external claws of second and third pair of legs and in the posterior claws of the hind legs (Figure 6M,N), considered by Biserov (1997/98) poorly visible. The characters of the type specimen examined correspond to the original description. We want to emphasise the presence of an increase of the thickness of the buccal tube wall after the stylet support insertion point (Figure 6I), and a LRU in the main branch of external claw on all legs (Figure 6L,M), not evidenced in the original description.

Ramazzottius edmondabouti Séméria, 1993

Due to the poor original description (Séméria 1993) of *R. edmondabouti*, it was not possible to verify the status of most of the characters useful to discriminate this species from the other species in the genus. For this reason and because of the unknown egg morphology of this species, we propose to assign to *R. edmondabouti* the status of *species dubia*, pending analyses of the type specimens (available at the Natural History Museum of Nice, France; Séméria et al. 2018).

Ramazzottius rupeus (Figure 7A-F)

The original description (Biserov 1999) provided drawings of the species and four LM photographs of the cuticle, claws and an egg. We provide new LM photographs of most taxonomic characters

considered in the species description derived from specimens different to those photographed by Biserov (1999). The characters of the type specimen examined correspond to the original description. We want to emphasise the presence a LRU in the main branch of external claw on all legs (Figure 7B), not evidenced in the original description.

Ramazzottius semisculptus **(Figure 7G-K)**

The original description (Pilato & Rebecchi 1992) provided only drawings of the species, we provide LM photographs of some taxonomic characters considered in the species description. The characters of the type specimen examined correspond to the original description. We want to emphasise the presence a LRU in the main branch of external claw on all legs (Figure 7I-K), not evidenced in the original description.

Ramazzottius subanomalus **(Figure 8A-E)**

The original description (Biserov 1985) provided drawings of the species and three LM photographs of the animals and an egg. We provide LM photographs of some taxonomic characters considered in the species description from type specimens already analysed by Stec et al. (2017) in the redescription of the species. We want to emphasise the presence a LRU in the main branch of the external claw on all legs (Figure 8B), not evidenced in previous descriptions (Biserov 1985; Stec et al. 2017).

Ramazzottius thulini **(Figure 8F-J)**

The original description (Pilato 1970) provided only drawings of the species, while some pictures of the type specimens were published in Pilato et al. (2013). We provide new LM photographs of the holotype, *in toto*, and of its bucco-pharyngeal apparatus and claws. The characters of the type specimen examined correspond to the original description. We want to emphasise the presence of an increase of the thickness of the buccal tube wall after the stylet support insertion point (Figure 8G), and a LRU in the main branch of external claw of all legs (Figure 8I,J), not evidenced in the original description.

Ramazzottius tribulosus **(Figure 9A-D)**

The original description (Bertolani & Rebecchi 1988) provided drawings of the species, one LM photograph of the egg, and one SEM picture of mouth opening. We provide new LM photographs of the bucco-pharyngeal apparatus, claws and an egg. The characters of the type specimen examined correspond to the original description. We want to emphasise the presence of a LRU in the main branch of external claw on all legs (Figure 9C,D), not evidenced in the original description.

Ramazzottius valaamis **(Figure 9E-I)**

The original description (Biserov & Tumanov 1993) provided drawings of the species and four LM photographs of the animals, feeding apparatus and eggs. We provide new LM photographs of the cuticle, bucco-pharyngeal apparatus, claws, and an egg (Figure 9E-I). We want to emphasise that contrary to the original description, a net-like sculpture is visible in the dorsal posterior cuticle (Figure 9I) in a paratype, and a LRU is present in the main branch of the external claw on all legs (Figure 9G).

Discussion

The discovery of a new species of *Ramazzottius*, observations of type materials hosted in public collections, and a review of the literature related to this genus led to an analysis of morphological characters within the genus and the comparison with other eutardigrades in an effort to understand their characteristics, distribution, and evolution.

Characteristics of the dorsal posterior cuticle

Ramazzottius kretschmanni sp. nov. has a smooth cuticle, but in most *Ramazzottius* species, the dorsal cuticle is characterized by small or large "bulges" (i.e. gibbosities, protuberances, tubercles), or even spines as in *Ramazzottius belubellus* Bartels, Nelson, Kaczmarek & Michalczyk, 2011b, or large hemispherical tubercles as in *R. saltensis* and *R. szeptycki* (which are absent in all the other species of the genus). When present, these "bulges" are always larger and more evident posteriorly.

Similar "bulges" in the dorsal posterior portion of the cuticle are present in many other species of different genera of Parachela (Eutardigrada) belonging to different evolutionary lineages and living in different environments and habitats. In these species, the posterior-dorsal cuticle (i.e. generally after the third pair of legs) is characterized by one of the following types of "bulges": gibbosities, granulations, tubercles, dots, crests, spines, outgrowths, and wrinkles. When these "bulges" are present in a more anterior-dorsal position, they are always reduced and/or less evident.

Although not exhaustive, the following taxa can be cited as representative of many evolutionary

lineages with such "bulges" in the posterior-dorsal cuticle: in Macrobiotoidea, the genera *Crenubiotus* (Richtersiusidae) and *Adorybiotus* (Adorybiotidae) and the species *Macrobiotus acadianus* (Meyer & Domingue, 2011), *Mesobiotus joenssoni* Guidetti, Gneuss, Cesari, Altiero & Schill, 2020, *Minibiotus ethelae* Claxton, 1998, and *Minibiotus aculeatus* (Murray, 1910) (Macrobiotidae); in Hypsibioidea, the genus *Cryoconicus*, most species of *Ramazzottius, Hebesuncus mollispinus* Pilato, McInnes & Lisi, 2012 (Ramazzottiidae), the genus *Calohypsibius* Thulin, 1928 (Calohypsibiidae), *Hypsibius scabropygus* Cuénot, 1929, *Pilatobius nodulosus* (Ramazzotti, 1957), *Platicrista brusoni* Miller & Miller, 2021 (Hypsibiidae); in Isohypsibioidea, the genus *Fractonotus* Pilato, 1998, the species *Thulinius romanoi* Bertolani, Bartels, Guidetti, Cesari & Nelson, 2014, *Thulinius gustavi* Massa, Guidetti, Cesari, Rebecchi & Jönsson, 2021, *Isohypsibius arbiter* Binda, 1980 (Isohypsibiidae), *Ursulinius elegans* (Binda & Pilato, 1971), *Grevenius monoicus* (Bertolani, 1982), *Doryphoribius zyxiglobus* (Horning, Schuster & Grigarick, 1978) (Doryphoribiidae), and *Ramajendas heatwolei* Miller Horning & Dastych, 1995.

The presence of a character that is similar in different unrelated phylogenetic lineages is considered the result of convergent evolution under similar selective pressure. Therefore, very probably there is a selective advantage for tardigrades to have an ornamented dorsal-posterior cuticle ("bulges").

A similar unknown selective pressure probably acts not only in Parachela, but also in limnoterrestrial Heterotardigrada, resulting in a similar phenomenon. In the heterotardigrades without cuticular plates, as e.g. *Orella mollis* Murray, 1910, there are posterior small gibbosities, while in the Echiniscidae with cuticular dorsal plates, the dorsal spines and/or filaments are in many cases present only on the posterior edge of the dorsal-posterior plates, and when other dorsal spines are present (except for the anterior sensory cirri), they are often smaller in size (e.g. see Guil 2008).

The possible selective pressure that led to this convergent evolution is unknown. Guidetti et al. (2019b) hypothesized that the dorsal-posterior granules in *Crenubiotus* species increase the animal's adhesion to the substrate, similar to the dot-like structures present on the legs of many Macrobiotoidea that very probably increase the grip of the leg on the substrate, but further data are needed to test this hypothesis. In tardigrades the ventral side of the body is always smooth and species of the same genus, living in similar habitats, can have different cuticular characteristics (e.g. the new species here described and other species of *Ramazzottius* have a smooth cuticle, although most species of the genus have an ornamented posterior cuticle). Other hypotheses to explain the phenomenon described could encompass cuticle permeability, sensory structures, hydrodynamics of the body, defence mechanisms, or it may not even be an adaptive trait and be caused by a non-adaptive developmental model.

Understanding the origin and function of these "bulges" will require more accurate phylogenetic analyses of genera and families. For example, our phylogenetic analysis for the *cox1* gene shows *Ramazzottius kretschmanni* sp. nov. in a basal position with respect of all other available *Ramazzottius* species (Figure 10), suggesting that a smooth cuticle could be the ancestral state. Given that this situation is not confirmed in the analysis of the ITS2 gene (Figure 11), a more accurate (molecular) phylogenetic analysis is required.

Gibbosities on the hind legs

According to Baumman (1966), Biserov (1985), and Rebecchi and Bertolani (1988), some *Ramazzottius* species have a lateral gibbosity (also called papillae or knobs) on each hind leg that is evident in males. These gibbosities (not always associated with the sex of the specimen) have been detected in *R. kretschmanni* (present study), *R. affinis* (this paper), *R. baumanni* (Ramazzotti 1962b), *R. conifer* (Ramazzotti & Maucci 1983), *R. tribulosus* (Rebecchi & Bertolani 1988), *R. agannae* (Dastych 2011), *Ramazzottius littoreus* Fontoura, Rubal & Veiga, 2017 (Fontoura et al. 2017), and *R. oberhaeuseri* (Stec et al. 2018), and in another population identified as *R. oberhaeuseri* (Baumann 1966). The same gibbosities are present in another genus in the same family Ramazzottiidae, i.e., *Cryoconicus* Zawierucha, Stec, Lachowska-Cierlik, Takeuchi, Li & Michalczyk, 2018; (Zawierucha et al. 2018; Guidetti et al. 2019b). Similar gibbosities on the hind legs have been reported only in males of some species of *Macrobiotus* Schultze, 1834 (e.g., Baumann 1970; Pilato et al. 2003; Fontoura et al. 2017; Stec et al. 2021). Therefore, the presence of these gibbosities on the hind legs of *Ramazzottius* species and their actual nature as a secondary sex character must be evaluated, as well as the taxonomic value of the character.

Head sensory regions

Ramazzottius kretschmanni sp. nov. has at least three sensory regions on the surface of the head, two of

which can be detected both with LM (Figure 1B,K) and SEM (Figure 3A, D) (i.e. peribuccal lobes and elliptical organs) and one only with SEM (i.e. cheek-like area; Figure 3C, E). Based on the relative position of these sensory regions, homologies with head sensory areas identified in other tardigrades (belonging to *Milnesium* Doyère, 1840, *Macrobiotus, Halobiotus* Kristensen, 1982) may be hypothesized (e.g. Walz 1978; Wiederhöft & Greven 1996; Wiederhöft & Greven 1999; Biserova & Kuznetsova 2012). The "peribuccal lobes" of *R. kretschmanni* (Figures 1K, 3D) correspond to the "circumoral sensory field" (COS) (a.k.a. peribuccal sense organ; Møbjerg et al. 2018), the "cheek-like area" (Figure 3E) to the "antero-lateral sensory field" (ALS), and the "elliptical organs" (Figure 1B) to the "postero-lateral sensory field" (PLS). These sensory regions are very probably conserved among eutardigrades (Wiederhöft & Greven 1999; Møbjerg et al. 2018).

All *Ramazzottius* species have the PLS (i.e., elliptical organs), while the "circumoral sensory field" is evident in *R. kretschmanni* sp. nov. (Figure 3D), *R. bunikowskae* (Kaczmarek et al. 2006), *R. agannae* (Dastych 2011), and *R. oberhaeuseri* (Stec et al. 2018). The size of each "peribuccal lobe" forming the COS appear asymmetrical around the mouth, with the three ventral lobes smaller than the three dorsal (Figures 3D, 4D; Kaczmarek et al. 2006; Dastych 2011; Stec et al. 2018). In *Milnesium* species (Apochela), there are six sensory papillae around the mouth; they correspond to the COS (Wiederhöft & Greven 1996, Wiederhöft & Greven 1999) and are homologous to the six peribuccal lobes of *Ramazzottius* (and *Crenubiotus* Lisi, Londoño & Quiroga, 2020, see below). Similar to the six peribuccal lobes, the six peribuccal papillae of *Milnesium* are not symmetrical in size, with the three ventral papillae smaller that the dorsal (e.g., see Figs in Guidetti et al. 2012; Morek et al. 2016, 2019a, 2019b, 2020a, 2020b).

Currently, the "antero-lateral sensory field" has been reported only in *R. kretschmanni* sp. nov. (Figure 3C) and *R. bunikowskae* (Kaczmarek et al. 2006). In *R. agannae*, the cuticular region corresponding to the "cheek-like" area in *R. kretschmanni* sp. nov. shows a different cuticular pattern (see Fig. 2 in Dastych 2011), indicating that this sensory area is also present in this species and probably in other species of the genus.

The organization of the COS into six lobes is also present in other species of the genera *Hebesuncus* Pilato, 1987 and *Cryoconicus* (see Dastych & Thaler 2002; Guidetti et al. 2019b, respectively), which also belong to the Ramazzottiidae. In particular, in *Cryoconicus antiarctos* Guidetti, Massa, Bertolani, Rebecchi & Cesari, 2019b, the "peribuccal lobes" (i.e. COS; Figure 4C), the "elliptical organs" (i.e. PLS; Figure 4E), and the "cheek-like" area (i.e. ALS; Figure 4 D,F,G) are visible in the head region. The presence of the three sensory regions in this species suggests that they can be also present in other taxa such as *Cryoconicus*, other members of Ramazzottiidae, and possibly in other eutardigrades.

Eye spots

Ramazzottius kretschmanni sp. nov. has no eye spots as in the other species of the genus, with the exception of *R. saltensis* and *Ramazzottius theroni* Dastych, 1993, which have eye spots. The presence of eyes is considered by Dastych (1993) as a plesiomorphic character within the genus.

After the recent revisions of eutardigrade genera (see Degma et al. 2021), the variability of morphological traits within each genus is very reduced, and generally the morphology of the animals among species of the same genus is very similar with usually only few and minute differences between them, but surprisingly, this is not the case regarding the presence of eye spots. In fact, other than *Ramazzottius*, other genera of eutardigrades have species with or without eye spots, for this reason the presence/absence of eye spots is used as taxonomic character: e.g. among the most abundant and widespread eutardigrade genera *Macrobiotus* (see Kaczmarek & Michalczyk 2017), *Paramacrobiotus* Guidetti, Schill, Bertolani, Dandekar & Wolf, 2009 (see Guidetti et al. 2019a), *Mesobiotus* Vecchi, Cesari, Bertolani, Jönsson, Rebecchi & Guidetti, 2016 (see Tumanov 2020), *Milnesium* (see Morek et al. 2016).

Eutardigrade eyes are positioned in the brain and may be termed as intracerebral photoreceptors. Although the evolution of vision in tardigrades is a complex phenomenon (Fleming et al. 2018), in the species studied so far, the eyes are composed of a single pigment-cup cell (with granules full of carotenoids; Bonifacio et al. 2012), a microvillous (i.e., rhabdomeric or retinula) cell, and one or two modified ciliary cells (Greven 2007).

It is very strange that such an important sensory structure as the eye could be lost or acquired so frequently during evolution. As suggested by Greven (2007), a possible explanation is the occurrence of light sensitive structures without shading pigments in the species that apparently do not have eye spots. Therefore, the species that do not show eye spots have the apparatus for vision but do not have the pigments within the cup-cell (or do not

have the cup-cell at all). This could explain the presence or absence of an eye spot even within a single specimen (Bąkowski et al. 2016). This hypothesis should be investigated in detail to evaluate the evolution of tardigrade vision and to determine the value of eye spots as a taxonomic trait.

Buccal tube walls

The buccal tube in *Ramazzottius* species is thin and relatively long. Posterior to the stylet support insertion, the buccal tube bends and has thicker walls that become thinner when it enters the pharynx (Figures 1D, 5A,L,M, Fig. 6I, 8G, 9A,E) [this thickening is not clearly visible and/or reported only in *Ramazzottius bunikowskae* Kaczmarek, Michalczyk & Diduszko, 2006, *Ramazzottius saltensis* (Claps & Rossi, 1984), *R. semisculptus* (Pilato & Rebecchi 1992), and *Ramazzottius szeptycki* (Dastych, 1980)]. The increasing in thickness of the buccal tube walls after the insertion point of the stylet support is also found in other species belonging to different evolutionary lineages: e.g., the species of the genera *Richtersius* Pilato & Binda, 1989 (Richtersiusidae), *Adorybiotus* Maucci & Ramazzotti, 1981 (Adrorybiotidae) and *Minibiotus* Schuster, 1980 in Schuster et al. 1980; (Guidetti et al. 2012, 2016), and in *Macrobiotus crustulus* Stec, Dudziak & Michalczyk, 2020a. This thickening is probably related to an unknown morpho-functional selective pressure that needs investigation.

Morphology of egg processes

The main morphological characters used to discriminate among *Ramazzottius* species are features related to egg morphology and dorsal cuticle ornamentation. Therefore, intraspecific variability in the egg processes can be an issue for species discrimination and identification as evidenced for *R. subanomalus* which can present a high variability of egg process morphology (Stec et al. 2016, 2017). The egg of *R. kretschmanni* sp. nov. is characterized by two types of processes: "hemispherical" (the most abundant) and "conical" (few and with variable shapes). In species of the "*oberhaeuseri* complex" (see above), the "hemispherical" egg processes maintain their shape, although they can differ in size and appearance on egg surface (Figure 2A-F; Pilato et al. 2013); while the shape of the "conical" process can vary greatly within each egg but are substantially similar between the species (see Figure 2H-J and Pilato et al. 2013, Stec et al. 2018). In *R. kretschmanni* sp. nov., the "conical" processes are responsible for the connection between two different eggs (Figure 2K-M), and their shape seems to be determined by the nature of this connection, e.g. the process can be pulled/stretched as in Figure 2K,L, or pushed/deformed as in Figure 2M. One hypothesis is that the "conical" processes are randomly present on the egg surface to increase the chance of touching and then connecting to another egg, and/or that they derived from "hemispherical" processes that have been deformed by the adhesion to other processes of a different egg. More information is needed to evaluate the true nature of the shape and numbers of the "conical" processes and their taxonomic value.

Acknowledgements

We would like to especially thank the Emeritus Prof. Diane Nelson for the English revision of the manuscript, and Prof. Lukasz Kaczmarek and the anonymous referee for their valuable suggestions. We also gratefully thank the Museo di Storia Naturale of Verona (Italy) and the museum curators Leonardo Latella and Roberta Salmaso for access to the Biserov, Maucci and Ramazzotti tardigrade collections and for the use of photos of the type specimens. We also appreciate the following colleagues: Dr. Denis Tumanov for information about *R. valaamis* and *R. subanomalus*; Prof. Giovanni Pilato, Prof. Maria Grazia Binda, and Prof. Oscar Lisi for their information and permission to use the photographs of type specimens in the Binda and Pilato collection; Prof. Oliver Betz and Monika Meinert for their support with the SEM pictures.

Disclosure statement

No potential conflict of interest was reported by the authors.

Supplementary material

Supplemental data for this article can be accessed here

ORCID

R. Guidetti http://orcid.org/0000-0001-6079-2538
M. Cesari http://orcid.org/0000-0001-8857-3791
L. Rebecchi http://orcid.org/0000-0001-5610-806X

References

Bąkowski M, Roszkowska M, Gawlak M, and Kaczmarek Ł. 2016. *Macrobiotus naskreckii* sp. nov., a new tardigrade (Eutardigrada: Macrobiotidae) of the *hufelandi* group from Mozambique. Annales Zoologici 66(2):155–164. DOI:10.3161/00034541ANZ2016.66.2.001.

Bartels PJ, Nelson DR, Exline RP. 2011a. Allometry and the removal of body size effects in the morphometric analysis of tardigrades. Journal of Zoological Systematics and Evolutionary Research 49(s1):17–25. DOI:10.1111/j.1439-0469.2010.00593.x.

Bartels PJ, Nelson DR, Kaczmarek Ł, and Michalczyk Ł. 2011b. *Ramazzottius belubellus*, a new species of Tardigrada (Eutardigrada: Parachela: Hypsibiidae) from the Great Smoky Mountains national park (North Carolina, U.S.A.). Proceedings of the Biological Society of Washington 124 (1):23–27. DOI:10.2988/10-13.1.

Baumann H. 1970. Lebenslauf und Lebensweise von *Macrobiotus hufelandi* Schultze (Tardigrada). Veröff. Überseemus. Bremen 4:29–43.

Baumman H. 1966. Der Lebenslauf von *Hypsibius* (*H.*) *oberhaeuseri* Doyère (Tardigrada). Veröeffentlichungen aus den Übersee-Museum, Bremen, Series A 3:245–258.

Bertolani R 1982. Tardigradi (Tardigrada). Guide per il riconoscimento delle specie animali delle acque interne italiane. Quaderni CNR, AQ/1/168, 15, 104 pp.

Bertolani R, Bartels PJ, Guidetti R, Cesari M, Nelson DR. 2014. Aquatic tardigrades in the Great Smoky Mountains National Park, North Carolina and Tennessee, USA, with the description of a new species of *Thulinius* (Tardigrada, Isohypsibiidae). Zootaxa 3764(5):524–536. DOI:10.11646/zootaxa.3764.5.2.

Bertolani R, Guidetti R, Rebecchi L. 1994. Tardigradi dell'Appennino umbro-marchigiano. Biogeographia 17:223–245.

Bertolani R, and Kinchin IM. 1993. A new species of *Ramazzottius* (Tardigrada, Hypsibiidae) in a rain gutter sediment from England. Zoological Journal of the Linnean Society 109(3):327–333. DOI:10.1111/j.1096-3642.1993.tb02538.x.

Bertolani R, Rebecchi L. 1988. The tardigrades of Emilia (Italy). I. Rossena. Bolletino di zoologia 55(1–4):367–371. DOI:10.1080/11250008809386634.

Binda MG. 1980. Tardigradi di Lucania. Animalia 7(1/3):79–91.

Binda MG, Pilato G. 1971. Nuovo contributo alla conoscenza dei Tardigradi di Sicilia. Bollettino dell'Accademia Gioenia di Scienze Naturali, Catania, Ser. 4a 10:896–909.

Binda MG, Pilato G. 1986. *Ramazzottius*, nuovo genere di eutardigrado (Hypsibiidae). Animalia 13:159–166.

Biserov VI. 1985. *Hypsibius subanomalus* sp. n. (Eutardigrada, Hypsibiidae) from the Astrakhan District. Zoologicheskii Zhurnal 64(1):131–135.

Biserov VI. 1997/98. Tardigrades of the Caucasus with a taxonomic analysis of the genus *Ramazzottius* (Parachela: Hypsibiidae). Zoologischer Anzeiger 236:139–159.

Biserov VI. 1999. A review of the Tardigrada from Novaya Zemlya; with descriptions of three new species and an evaluation of the state of the environment in this region. Zoologischer Anzeiger 238:169–182.

Biserov VI, Trumanov DV. 1993. *Ramazzottius valaamis* sp. n. (Tardigrada, Hypsibiidae), a new species of tardigrade from Valaam Island, Karelia, Russia. Zoologichesky Zhurnal 72:35–39.

Biserova NM, Kuznetsova KG. 2012. Head sensory organs of *Halobiotus stenostomus* (Eutardigrada, Hypsibiidae). Biology Bulletin 39(7):579–589. DOI:10.1134/S1062359012070035.

Bonifacio A, Guidetti R, Altiero T, Sergo V, Rebecchi L. 2012. Nature, source and function of pigments in tardigrades: In vivo Raman imaging of carotenoids in *Echiniscus blumi*. PLoS One 7(11):e50162. DOI:10.1371/journal.pone.0050162.

Cesari M, Bertolani R, Rebecchi L, Guidetti R. 2009. DNA barcoding in Tardigrada: The first case study on *Macrobiotus macrocalix* Bertolani & Rebecchi 1993 (Eutardigrada, Macrobiotidae). Molecular Ecology Resources 9 (3):699–706. DOI:10.1111/j.1755-0998.2009.02538.x.

Cesari M, Giovannini I, Bertolani R, Rebecchi L. 2011. An example of problems associated with DNA barcoding in tardigrades: A novel method for obtaining voucher specimens. Zootaxa 3104(1):42–51. DOI:10.11646/zootaxa.3104.1.3.

Claps MC, Rossi GC. 1984. Contribucíon al conocimiento de los Tardigrados de Argentina. IV. Acta Zoologica Lilloana 38:45–50.

Claxton SK. 1998. A revision of the genus *Minibiotus* (Tardigrada: Macrobiotidae) with descriptions of eleven new species from Australia. Records of the Australian Museum 50 (2):125–160. DOI:10.3853/j.0067-1975.50.1998.1276.

Clement M, Posada D, Crandall K. 2000. TCS: A computer program to estimate gene genealogies. Molecular Ecology 9 (10):1657–1660. DOI:10.1046/j.1365-294x.2000.01020.x.

Cuénot L. 1929. Description d'un tardigrade nouveau de la faune francaise. Archives D'anatomie Microscopique 25:121–125.

Darriba D, Taboada GL, Doallo R, Posada D. 2012. jModelTest 2: More models, new heuristics and parallel computing. Nature Methods 9(8):772. DOI:10.1038/nmeth.2109.

Dastych H. 1980. *Hypsibius szeptycki* sp. nov., a new species of Tardigrada from South Africa. Bulletin of the Polish Academy of Sciences 27(6):505–508. Warszawa.

Dastych H. 1983. Two new Eutardigrada species from West Spitsbergen and the Tatra Mts. Bulletin de la Société des amis des sciences et des lettres de Poznań 23:195–200.

Dastych H. 1993. A new genus and four new species of semiterrestrial water-bears from South Africa (Tardigrada). Mitteilungen aus dem Hamburgischen Zoologischen Museum und Institut 90:175–186.

Dastych H. 2011. *Ramazzottius agannae* sp. nov., a new tardigrade species from the nival zone of the Austrian Central Alps (Tardigrada). Entomologische Mitteilungen aus dem Zoologischen Museum Hamburg 15(186):237–253.

Dastych H, Thaler K. 2002. The tardigrade *Hebesuncus conjungens* (Thulin, 1911) in the Alps, with notes on morphology and distribution (Tardigrada). Emtomologische Mitteilungen aus dem Zoologischen Museum, Hamburg 14(166):83–94.

Degma P, Bertolani R, Guidetti R 2021. Actual checklist of Tardigrada species. DOI: 10.25431/11380_1178608. Accessed date: 06/08/2021.

Doyère LMF. 1840. Memoire sur les Tardigrades. I. Annales Des Sciences Naturelles, Paris, Series 2(14):269–362.

Faurby S, Jönsson KI, Rebecchi L, Funch P. 2008. Variation in anhydrobiotic survival of two eutardigrade morphospecies: A story of cryptic species and their dispersal. Journal of Zoology 275(2):139–145. DOI:10.1111/j.1469-7998.2008.00420.x.

Fleming JF, Kristensen RM, Sørensen MV, Park TYS, Arakawa K, Blaxter M, Rebecchi L, Guidetti R, Williams TA, Roberts NW, Vinther J, Pisani D. 2018. Molecular palaeontology illuminates the evolution of ecdysozoan vision. Proceedings of the Royal Society B 285 (1892):20182180. DOI:10.1098/rspb.2018.2180.

Fontoura P, Rubal M, Veiga P. 2017. Two new species of Tardigrada (Eutardigrada: Ramazzottiidae, Macrobiotidae) from the supralittoral zone of the Atlantic Iberian Peninsula rocky shores. Zootaxa 4263(3):450–466. DOI:10.11646/zootaxa.4263.3.2.

Gąsiorek P, Jackson KJ, Meyer HA, Zając K, Nelson DR, Kristensen RM, and Michalczyk Ł. 2019. *Echiniscus virginicus* complex: The first case of pseudocryptic allopatry and pantropical distribution in tardigrades. Biological Journal of the Linnean Society 128(4):789–805. DOI:10.1093/biolinnean/blz147

Gąsiorek P, Stec D, Morek W, Michalczyk Ł. 2018. An integrative redescription of *Hypsibius dujardini* (Doyère, 1840), the nominal taxon for Hypsibioidea (Tardigrada: Eutardigrada). Zootaxa 4415(1):45–75. DOI:10.11646/zootaxa.4415.1.2.

Greven H. 2007. Comments on the eyes of tardigrades. Arthropod Structure & Development 36(4):401–407. DOI:10.1016/j.asd.2007.06.003.

Guidetti R, Altiero T, Marchioro T, Amade LS, Avdonina AM, Bertolani R, Rebecchi L. 2012. Form and function of the feeding apparatus in Eutardigrada (Tardigrada). Zoomorphology 131(2):127–148. DOI:10.1007/s00435-012-0149-0.

Guidetti R, Cesari M, Bertolani R, Altiero T, Rebecchi L. 2019a. High diversity in species, reproductive modes and distribution within the *Paramacrobiotus richtersi* complex (Eutardigrada, Macrobiotidae). Zoological Letters 5(1):1–28. DOI:10.1186/s40851-018-0113-z.

Guidetti R, Gneuß E, Cesari M, Altiero T, and Schill RO. 2020. Life-history traits and description of the new gonochoric amphimictic *Mesobiotus joenssoni* (Eutardigrada: Macrobiotidae) from the Island of Elba, Italy. Zoological Journal of the Linnean Society 188(3):848–859. DOI:10.1093/zoolinnean/zlz077

Guidetti R, Massa E, Bertolani R, Rebecchi L, Cesari M. 2019b. Increasing knowledge of Antarctic biodiversity: New endemic taxa of tardigrades (Eutardigrada; Ramazzottiidae) and their evolutionary relationships. Systematics and Biodiversity 17 (6):573–593. DOI:10.1080/14772000.2019.1649737.

Guidetti R, Rebecchi L, Bertolani R, Jönsson KI, Møbjerg Kristensen R, Cesari M. 2016. Morphological and molecular analyses on *Richtersius* (Eutardigrada) diversity reveal its new systematic position and lead to the establishment of a new genus and a new family within Macrobiotoidea. Zoological Journal of the Linnean Society 178(4):834–845. DOI:10.1111/zoj.12428.

Guidetti R, Schill RO, Bertolani R, Dandekar T, and Wolf M. 2009. New molecular data for tardigrade phylogeny, with the erection of *Paramacrobiotus* gen. nov. Journal of Zoological Systematics and Evolutionary Research 47(4):315–321. DOI:10.1111/j.1439-0469.2009.00526.x.

Guidetti R, Schill RO, Giovannini I, Massa E, Goldoni SE, Ebel C, Förschler MI, Rebecchi L, and Cesari M. 2021. When DNA sequence data and morphological results fit together: Phylogenetic position of *Crenubiotus* within Macrobiotoidea (Eutardigrada) with description of *Crenubiotus ruhesteini* sp. nov. Journal of Zoological Systematics and Evolutionary Research 59 (3):576–587. DOI:10.1111/jzs.12449.

Guil N. 2008. New records and within-species variability of Iberian tardigrades (Tardigrada), with comments on the species from the *Echiniscus blumi-canadensis* series. Zootaxa 1757 (1):1–30. DOI:10.11646/zootaxa.1757.1.1.

Guil N, Giribet G. 2009. Fine scale population structure in the *Echiniscus blumi-canadensis* series (Heterotardigrada, Tardigrada) in an Iberian mountain range—When morphology fails to explain genetic structure. Molecular Phylogenetics and Evolution 51 (3):606–613. DOI:10.1016/j.ympev.2009.02.019.

Guindon S, Gascuel O. 2003. A simple, fast and accurate method to estimate large phylogenies by maximum-likelihood. Systematic Biology 52(5):696–704. DOI:10.1080/10635150390235520.

Hart MW, Sunday J. 2007. Things fall apart: Biological species form unconnected parsimony networks. Biology Letters 3 (5):509–512. DOI:10.1098/rsbl.2007.0307.

Horning Jr DS, Schuster RO, Grigarick AA. 1978. Tardigrada of New Zealand. New Zealand Journal of Zoology 5 (2):185–280. DOI:10.1080/03014223.1978.10428316.

Huelsenbeck JP, Ronquist F. 2001. MRBAYES: Bayesian inference of phylogenetic trees. Bioinformatics 17(8):754–755. DOI:10.1093/bioinformatics/17.8.754.

Kaczmarek Ł, Michalczyk Ł. 2017. The *Macrobiotus hufelandi* group (Tardigrada) revisited. Zootaxa 4363(1):101–123. DOI:10.11646/zootaxa.4363.1.4.

Kaczmarek Ł, Michalczyk Ł, Diduszko D. 2006. *Ramazzottius bunikowskae*, a new species of Tardigrada (Eutardigrada, Hypsibiidae) from Russia. Zootaxa 1229(1):49–57. DOI:10.11646/zootaxa.1229.1.4.

Kaczmarek Ł, Michalczyk Ł, McInnes SJ. 2014. Annotated zoogeography of non-marine Tardigrada. Part I: Central America. Zootaxa 3763(1):1–62. DOI:10.11646/zootaxa.3763.1.1.

Kaczmarek Ł, Michalczyk Ł, McInnes SJ. 2015. Annotated zoogeography of non-marine Tardigrada. Part II: South America. Zootaxa 3923(1):001–107. DOI:10.11646/zootaxa.3923.1.1.

Kaczmarek Ł, Michalczyk Ł, McInnes SJ. 2016. Annotated zoogeography of non-marine Tardigrada. Part III: North America and Greenland. Zootaxa 4203(1):1–249. DOI:10.11646/zootaxa.4203.1.1.

Kaczmarek Ł, Roszkowska M, Poprawa I, Janelt K, Kmita H, Gawlak M, Fiałkowska E, Mioduchowska M. 2020. Integrative description of bisexual *Paramacrobiotus experimentalis* sp. nov. (Macrobiotidae) from republic of Madagascar (Africa) with microbiome analysis. Molecular Phylogenetics and Evolution 145:106730. DOI:10.1016/j.ympev.2019.106730.

Katoh K, Misawa K, Kuma KI, Miyata T. 2002. MAFFT: A novel method for rapid multiple sequence alignment based on fast Fourier transform. Nucleic Acids Research 30 (14):3059–3066. DOI:10.1093/nar/gkf436.

Katoh K, Rozewicki J, Yamada KD. 2017. MAFFT online service: Multiple sequence alignment, interactive sequence choice and visualization. Briefings in Bioinformatics 108. DOI: 10.1093/bib/bbx108.

Kihm JH, Kim S, McInnes SJ, Zawierucha K, Rho HS, Kang P, Park TYS. 2020. Integrative description of a new *Dactylobiotus* (Eutardigrada: Parachela) from Antarctica that reveals an intraspecific variation in tardigrade egg morphology. Scientific Reports 10(1):1–11. DOI:10.1038/s41598-020-65573-1.

Kristensen RM. 1982. The first record of cyclomorphosis in Tardigrada based on a new genus and species from Arctic meiobenthos. Z. Zool. Systematic Evolut.- Forsh 20:249–270. DOI:10.1111/j.1439-0469.1983.tb00552.x.

Kumar S, Stecher G, Li M, Knyaz C, Tamura K. 2018. MEGA X: Molecular Evolutionary Genetics Analysis across Computing Platforms. Molecular Biology and Evolution 35 (6):1547–1549. DOI:10.1093/molbev/msy096.

Lisi O, Londoño R, Quiroga S. 2020. Description of a new genus and species (Eutardigrada: Richtersiidae) from Colombia, with comments on the family Richtersiidae. Zootaxa 4822 (4):531–550. DOI:10.11646/zootaxa.4822.4.4.

Massa E, Guidetti R, Cesari M, Rebecchi L, Jönsson KI. 2021. Tardigrades of Kristianstads Vattenrike Biosphere Reserve with description of four new species from Sweden. Scientific Reports 11(1):1–19. DOI:10.1038/s41598-021-83627-w.

Maucci W, and Ramazzotti G. 1981. *Adorybiotus* gen. nov.: Nuova posizione sistematica per *Macrobiotus granulatus* Richters, 1903 e per *Macrobiotus coronifer* Richters, 1903 (Tardigrada, Macrobioitdae). Memorie dell'Istituo Italiano di Idrobiologia 39:153–159.

McInnes SJ. 1994. Zoogeographic distribution of terrestrial/freshwater tardigrades from current literature. Journal of Natural History 28(2):257–352.

McInnes SJ, Michalczyk Ł, Kaczmarek Ł. 2017. Annotated zoogeography of non-marine Tardigrada. Part IV: Africa. Zootaxa 4284(1):1–74. DOI:10.11646/zootaxa.4284.1.1.

Meyer HA, and Domingue MN. 2011. *Minibiotus acadianus* (Eutardigrada: Macrobiotidae), ANew Species of Tardigrada from Southern Louisiana, U.S.A. Western North American Naturalist 71(1):38–43. DOI:10.3398/064.071.0106.

Michalczyk Ł, Kaczmarek Ł. 2013. The Tardigrada Register: A comprehensive online data repository for tardigrade taxonomy. Journal of Limnology 72(1s):175–181. DOI:10.4081/jlimnol.2013.s1.e22.

Miller WR, Horning DS, and Dastych H. 1995. Tardigrades of the Australian Antarctic: Description of two new species from Macquarie Island, Subantarctica. Entomologische Mitteilungen aus dem Zoologischen Museum 11 (152):231–239.

Miller WR, Miller JD. 2021. Tardigrades of North America: *Platicrista brunsoni* nov. sp. (Parachela, Hypsibiidae, Itaquasconinae) from the Bob Marshall Wilderness Area of Montana. Northwest Science 95(1):98–105. DOI:10.3955/046.095.0106.

Miller MA, Pfeiffer W, Schwartz T. 2010. Creating the CIPRES Science Gateway for inference of large phylogenetic trees. 2010 Gateway Computing Environments Workshop (GCE) 1–8.

Møbjerg N, Jørgensen A, Kristensen RM, Neves RC. 2018. Morphology and functional anatomy. In: Schill R, editor. Water bears: The biology of tardigrades. Cham: Springer. pp. 57–94.

Morek W, Blagden B, Kristensen RM, Michalczyk Ł. 2020b. The analysis of inter- and intrapopulation variability of *Milnesium eurystomum* Maucci, 1991 reveals high genetic divergence and a novel type of ontogenetic variation in the order Apochela. Systematics and Biodiversity 18(6):614–632. DOI:10.1080/14772000.2020.1771469.

Morek W, Gąsiorek P, Stec D, Blagden B, Michalczyk Ł. 2016. Experimental taxonomy exposes ontogenetic variability and elucidates the taxonomic value of claw configuration in *Milnesium* Doyère, 1840 (Tardigrada: Eutardigrada: Apochela). Contributions to Zoology 85(2):173–200. DOI:10.1163/18759866-08502003.

Morek W, Stec D, Gąsiorek P, Surmacz B, Michalczyk Ł. 2019a. *Milnesium tardigradum* Doyère, 1840: The first integrative study of interpopulation variability in a tardigrade species. Journal of Zoological Systematics and Evolutionary Research 57(1):1–23. DOI:10.1111/jzs.12233.

Morek W, Surmacz B, Michalczyk Ł. 2020a. Novel integrative data for two *Milnesium* Doyère, 1840 (Tardigrada: Apochela) species from Central Asia. Zoosystematics and Evolution 96 (2):499–514. DOI:10.3897/zse.96.52049.

Morek W, Suzuki AC, Schill RO, Georgiev D, Yankova M, Marley NJ, Michalczyk Ł. 2019b. Redescription of *Milnesium alpigenum* Ehrenberg, 1853 (Tardigrada: Apochela) and a description of *Milnesium inceptum* sp. nov., a tardigrade laboratory model. Zootaxa 4586(1):35–64. DOI:10.11646/zootaxa.4586.1.2.

Múrias Dos Santos A, Cabezas MP, Tavares AI, Xavier R, Branco M. 2016. tcsBU: A tool to extend TCS network layout and visualization. Bioinformatics 32(4):627–628. DOI:10.1093/bioinformatics/btv636.

Murray J. 1910. Tardigrada. British Antarctic Expedition 1907–9. Reports on the Scientific Investigations. Volume 1 Biology Part V:81–185.

Nelson DR, Fletcher RA, Guidetti R, Roszkowska M, Grobys D, and Kaczmarek Ł. 2020. Two new species of Tardigrada from moss cushions (*Grimmia* sp.) in a xerothermic habitat in northeast Tennessee (USA, North America), with the first identification of males in the genus *Viridiscus*. PeerJ 8: e10251. DOI:10.7717/peerj.10251.

Nylander JAA. 2004. MrModeltest v2. Program distributed by the author. Evolutionary Biology Centre, Uppsala University, Uppsala, Sweden.

Pilato G. 1970. Osservazioni sui Tardigradi delle Alpi Apuane. Lavori della Società Italiana di Biogeografia 1:336–348.

Pilato G. 1987. Revision of the genus *Diphascon* Plate, 1889, with remarks on the subfamily Itaquasconinae (Eutardigrada, Hypsibiidae). In: Bertolani R, editor. Biology of Tardigrades, Vol. 1. Mucchi, Modena: U.Z.I., 337–357. Selected Symposia and Monographs.

Pilato G. 1998. Microhypsibiidae, new family of eutardigrades, and description of the new genus *Fractonotus* (Tardigrada). Spixiana 21:129–134.

Pilato G, Binda MG. 1989. *Richtersius*, nuovo nome generico in sostituzione di *Richtersia* Pilato e Binda, 1987 (Eutardigrada). Animalia 16:147–148.

Pilato G, D'Urso V, Lisi O. 2013. *Ramazzottius thulini* (Pilato, 1970) *bona* species and description of *Ramazzottius libycus* sp. nov. (Eutardigrada, Ramazzottidae). Zootaxa 3681 (3):270–280. DOI:10.11646/zootaxa.3681.3.6.

Pilato G, Kaczmarek Ł, Michalczyk Ł, and Lisi O. 2003. *Macrobiotus polonicus*, a new species of Tardigrada from Poland (Eutardigrada: Macrobiotidae, '*hufelandi* group'). Zootaxa 258(1):1–8. DOI:10.11646/zootaxa.258.1.1.

Pilato G, McInnes SJ, Lisi O. 2012. *Hebesuncus mollispinus* (Eutardigrada, Hypsibiidae), a new species from maritime Antarctica. Zootaxa 3446(1):60–68. DOI:10.11646/zootaxa.3446.1.4.

Pilato G, Rebecchi L. 1992. *Ramazzottius semisculptus*, nuova specie di Hypsibiidae (Eutardigrada). Animalia 19:227–234.

Puillandre N, Brouillet S, Achaz G. 2021. ASAP: Assemble species by automatic partitioning. Molecular Ecology Resources 21(2):609–620. DOI:10.1111/1755-0998.13281.

Ramazzotti G. 1957. Due nuove specie di Tardigradi extra-europei. Atti della Società Italiana di Scienze Naturali, Museo Civico di Storia Naturale, Milano 96:188–191.

Ramazzotti G. 1962a. Il Phylum Tardigrada. Memorie dell'Istituto Italiano di Idrobiologia XVI:1–595.

Ramazzotti G. 1962b. Tardigradi del Cile, con descrizione di quattro nuove specie e di una nuova varietà. Atti della Società Italiana di Scienze Naturali, Museo Civico di Storia Naturale, Milano 101:275–287.

Ramazzotti G, and Maucci W. 1983. Il Phylum Tardigrada. III Edizione riveduta e aggiornata. Memorie dell'Istituto Italiano di Idrobiologia 41: 1–1012.

Rambaut A, Drummond AJ, Xie D, Baele G, Suchard MA. 2018. Posterior Summarization in Bayesian Phylogenetics Using Tracer 1.7. Systematic Biology 67(5):901–904. DOI:10.1093/sysbio/syy032.

Rebecchi L, Bertolani R. 1988. The tardigrades of Emilia (Italy). I. Rossena. Italian Journal of Zoology 55:367–371.

Ronquist F, Huelsenbeck JP. 2003. MrBayes 3: Bayesian phylogenetic inference under mixed models. Bioinformatics 19 (12):1572–1574. DOI:10.1093/bioinformatics/btg180.

Santos E, Veiga P, Rubal M, Bartels PJ, Cmc DR, Fontoura P. 2019. *Batillipes pennaki* Marcus, 1946 (Arthrotardigrada: Batillipedidae): Deciphering a species complex. Zootaxa 4648(3):549–567. DOI:10.11646/zootaxa.4648.3.9.

Schill RO, Förster F, Dandekar T, Wolf M. 2010. Using compensatory base change analysis of internal transcribed spacer 2 secondary structures to identify three new species in

Paramacrobiotus (Tardigrada). Organisms Diversity & Evolution 10(4):287–296. DOI:10.1007/s13127-010-0025-z.

Schill RO, Steinbrück G. 2007. Identification and differentiation of Heterotardigrada and Eutardigrada species by riboprinting. Journal of Zoological Systematics and Evolutionary Research 45(3):184–190. DOI:10.1111/j.1439-0469.2007.00409.x.

Schultze CAS, 1834. *Macrobiotus Hufelandii* animal e crustaceorum classe novum, reviviscendi post diuturnam asphixiam et aridiatem potens. 8, 1 tab. C. Curths, Berlin, 6 pp, I Table.

Schuster RO, Nelson DR, Grigarick AA, Christenberry D. 1980. Systematic criteria of the Eutardigrada. Trans. Am. Micros. Soc 99:284–303. DOI:10.2307/3226004.

Séméria Y. 1993. Description d'une espèce nouvelle de Tardigrade du Vénézuéla, *Ramazzottius edmondabouti* n. sp. (Eutardigrada, Hypsibiidae). Bulletin Mensuel de la Société Linnéenne de 62:215–216.

Séméria Y, Gerriet O, Lambert G. 2018. La collection de tardigrades Yves Séméria du Muséum d'Histoire naturelle de Nice (France). Biocosme Mésogéen 35(3–4):27–42.

Stamatakis A. 2006. RAxML-VI-HPC: Maximum likelihood-based phylogenetic analyses with thousands of taxa and mixed models. Bioinformatics 22(21):2688–2690. DOI:10.1093/bioinformatics/btl446.

Stamatakis A, Hoover P, Rougemont J. 2008. A rapid bootstrap algorithm for the RAxML web servers. Systematic Biology 57 (5):758–771. DOI:10.1080/10635150802429642.

Stec D, Dudziak M, and Michalczyk Ł. 2020a. Integrative descriptions of two new Macrobiotidae species (Tardigrada: Eutardigrada: Macrobiotoidea) from French Guiana and Malaysian Borneo. Zoological Studies 59:23. DOI:10.6620/ZS.2020.59-23

Stec D, Kristensen RM, and Michalczyk Ł. 2020b. An integrative description of *Minibiotus ioculator* sp. nov. from the Republic of South Africa with notes on *Minibiotus pentannulatus* Londoño et al., 2017 (Tardigrada: Macrobiotidae). Zoologischer Anzeiger 286:117–134. DOI:10.1016/j.jcz.2020.03.007.

Stec D, Morek W, Gąsiorek P, Kaczmarek Ł, Michalczyk Ł. 2016. Determinants and taxonomic consequences of extreme egg shell variability in *Ramazzottius subanomalus* (Biserov, 1985) (Tardigrada). Zootaxa 4208(2):176–188. DOI:10.11646/zootaxa.4208.2.5.

Stec D, Morek W, Gąsiorek P, Michalczyk Ł. 2018. Unmasking hidden species diversity within the Ramazzottius oberhaeuseri complex, with an integrative redescription of the nominal species for the family Ramazzottiidae (Tardigrada: Eutardigrada: Parachela). Systematics and Biodiversity 16 (4):357–376. DOI:10.1080/14772000.2018.1424267.

Stec D, Vecchi M, Dudziak M, Bartels PJ, Calhim S, Michalczyk Ł. 2021. Integrative taxonomy resolves species identities within the *Macrobiotus pallarii* complex (Eutardigrada: Macrobiotidae). Zoological Letters 7 (1):1–45. DOI:10.1186/s40851-021-00176-w.

Stec D, Zawierucha K, Michalczyk Ł. 2017. An integrative description of *Ramazzottius subanomalus* (Biserov, 1985 (Tardigrada) from Poland. Zootaxa 4300(3):403–420. DOI:10.11646/zootaxa.4300.3.4.

Templeton AR, Crandall KA, Sing CF. 1992. A cladistic analysis of phenotypic association with haplotypes inferred from restriction endonuclease mapping and DNA sequence data. III. Cladogram Estimation. Genetics 132(2):619–633.

Thulin G. 1928. Über die Phylogenie und das System der Tardigraden. Hereditas 11(2–3):207–266. DOI:10.1111/j.1601-5223.1928.tb02488.x.

Tumanov DV. 2020. Integrative description of *Mesobiotus anastasiae* sp. nov. (Eutardigrada, Macrobiotoidea) and first record of *Lobohalacarus* (Chelicerata, Trombidiformes) from the Republic of South Africa. European Journal of Taxonomy 726:102–131. DOI:10.5852/ejt.2020.726.1179.

Urbanowicz C. 1925. Sur la variabilit de *Macrobiotus oberhaeuseri*. Bulletin biologique de la France et de la Belgique 59:124–142.

Vecchi M, Cesari M, Bertolani R, Jönsson KI, Rebecchi L, Guidetti R. 2016. Integrative systematic studies on tardigrades from Antarctica identify new genera and new species within Macrobiotoidea and Echiniscoidea. Invertebrate Systematics 30(4):303–322. DOI:10.1071/IS15033.

Walz B. 1978. Electron microscopic investigation of cephalic sense organs of the tardigrade *Macrobiotus hufelandi* C.A.S. Schultze. Zoomorphologie 89(1):1–19. DOI:10.1007/BF00993778.

Wełnicz W, Grohme MA, Kaczmarek Ł, Schill RO, and Frohme M. 2011. ITS-2 and 18S rRNA data from *Macrobiotus polonicus* and *Milnesium tardigradum* (Eutardigrada, Tardigrada). Journal of Zoological Systematics and Evolutionary Research 49(s1):34–39. DOI:10.1111/j.1439-0469.2010.00595.x.

Wiederhöft H, and Greven H. 1999. Notes on head sensory organs of *Milnesium tardigradum* Doyre, 1840 (Apochela, Eutardigrada). Zoologischer Anzeiger 238(3–4):338–346.

Wiederhöft H, Greven H. 1996. The cerebral ganglia of *Milnesium tardigradum* Doyère (Apochela, Tardigrada): Three dimensional reconstruction and notes on their ultrastructure. Zoological Journal of the Linnean Society 116(1–2):71–84. DOI:10.1111/j.1096-3642.1996.tb02334.x.

Zawierucha K, Stec D, Lachowska-Cierlik D, Takeuchi N, Li Z, and Michalczyk Ł. 2018. High mitochondrial diversity in a new water bear species (Tardigrada: Eutardigrada) from mountain glaciers in central asia, with the erection of a new genus *Cryoconicus*. Annales Zoologici 68(1):179–201. DOI:10.3161/00034541ANZ2018.68.1.007.

Zhang J, Kapli P, Pavlidis P, Stamatakis A. 2013. A general species delimitation method with applications to phylogenetic placements. Bioinformatics 29(22):2869–2876. DOI:10.1093/bioinformatics/btt499.